Published in final edited form as:
Neuroscience. 2008 June 12; 154(1): 29–50. doi:10.1016/j.neuroscience.2008.01.035.

Distribution and phenotypes of unipolar brush cells in relation to the granule cell system of the rat cochlear nuclear nucleus

Maria. R. Diño and **Enrico Mugnaini**
Department of Cellular and Molecular Biology, The Feinberg School of Medicine, Northwestern University, Searle 5-474, 320 E. Superior Street, Chicago IL 60611

Abstract

In most mammals the cochlear nuclear complex (CN) contains a distributed system of granule cells (GCS), whose parallel fiber axons innervate the dorsal cochlear nucleus (DCN). Like their counterpart in cerebellum, CN granules are innervated by mossy fibers of various origins. The GCS is complemented by unipolar brush (UBCs) and Golgi cells, and by stellate and cartwheel cells of the DCN. This cerebellum-like microcircuit modulates the activity of the DCN's main projection neurons, the pyramidal, giant and tuberculoventral neurons, and is thought to improve auditory performance by integrating acoustic and proprioceptive information. In this paper, we focus on the UBCs, a chemically heterogeneous neuronal population, using antibodies to calretinin, mGluR1α epidermal growth factor substrate 8 (Eps8) and the transcription factor Tbr2. Eps8 and Tbr2 labeled most of the CN's UBCs, if not the entire population, while calretinin and mGluR1α distinguished two largely separate subsets with overlapping distributions. By double labeling with antibodies to Tbr2 and the α6 $GABA_A$-receptor subunit, we found that UBCs populate all regions of the GCS and occur at remarkably high densities in the DCN and subpeduncular corner, but rarely in the lamina. Although GCS subregions likely share the same microcircuitry, their dissimilar UBC densities suggest they may be functionally distinct. UBCs and granules are also present in regions previously not included in the GCS, namely the rostrodorsal magnocellular portions of VCN, vestibular nerve root, trapezoid body, spinal tract and sensory and principal nuclei of the trigeminal nerve, and cerebellar peduncles. The UBC's dendritic brush receives AMPA- and NMDA-mediated input from an individual mossy fiber, favoring singularity of input, and its axon most likely forms several mossy fiber-like endings that target numerous granule cells and other UBCs, as in the cerebellum. The UBCs therefore, may amplify afferent signals temporally and spatially, synchronizing pools of target neurons.

Keywords

Eps8; Tbr2; auditory performance; subunit α6 $GABA_A$ receptor; calretinin; mGluR1α

The cochlear nuclear complex (CN) is the primary center of the auditory brainstem and the site of termination of all spiral ganglion fibers; in addition to the cochlear nerve, it receives afferent fibers from multiple sources via three routes, the dorsal, intemediate, and ventral acoustic striae,

Corresponding Author: Enrico Mugnaini, Department of Cellular and Molecular Biology, The Feinberg School of Medicine, Northwestern University, Searle 5-474, 320 E. Superior Street, Chicago IL 60611, e-mugnaini@northwestern.edu.
Section Editor: O. P. Ottersen (Special Issue: Auditory Neuroscience)

which are also channels for its efferent projections. An intriguing aspect of CN organization in mammals is the highly diverse structure of its nuclear subdivisions, which consists in the ventral (VCN) and dorsal (DCN) cochlear nuclei and the granule cell system (Ryugo and Parks, 2003).

The mammalian VCN and DCN are reciprocally connected and differ in neuronal organization and projection patterns (Osen, 1969; Lorente de Nó, 1981; Brawer et al., 1974; Cant, 1992; Cant and Benson, 2003; Malmierca, 2003; Young and Oertel, 2004). Except for a thin outer region made up of small neurons, the VCN is a predominantly magnocellular nucleus whose large neurons form multiple projections that innervate primarily the superior olivary complex and lateral lemniscal nuclei, and also the inferior colliculus and contralateral CN; in rodents, the auditory nerve root house a special group of large VCN neurons, whose axons project to the pontine reticular formation establishing the first link of the acoustic startle reflex (reviewed by Gómez-Nieto et al., 2007). By contrast, the DCN has a trilaminar structure consisting of: a molecular layer, which contains scattered small neurons; a layer containing the cell bodies of large, pyramidal (or fusiform) projection neurons; and a polymorphic layer (or deep region), which contains the basal dendrites of the pyramidal cells and several types of varysized neurons, including a small number of giant cells. The main targets of the DCN neurons are the inferior colliculus and part of the medial geniculate body (Anderson et al., 2006). That VCN and DCN derive from different rhombomeric regions of the hindbrain's lower rhombic lip (Farago et al., 2006) further highlights their different cytoarchitecture. Genes with preferred expression in the major CN subdivisions have also been identified (Friedland et al., 2006; Saul et al., 2007).

The mammalian CN also contains bands and clusters of granule cells distributed in both VCN and DCN divisions and collectively referred to as the "granule cell domain" or "granule cell system" (GCS) (Mugnaini et al., 1980a,b; Osen and Mugnaini, 1981; Lorente de Nó, 1981; Hackney et al., 1990). The granule bands are so prominent in many species that they are considered by some to form a third CN division. Although its presence in cetacea and anthropoid and human primates is debated (Osen and Jansen, 1965; Moskowitz, 1969; Strominger, 1978; Moore and Osen, 1979; Moore, 1980, 1987; Webster, 1992), the GCS represents a substantial CN component in most mammalian species. Because their axons converge on the molecular layer of the DCN, the granule cells and their afferents are believed to form a functionally unique system within the CN (Mugnaini et al., 1980b; Dunn et al., 1996; Oertel and Young, 2004) that is thought to improve auditory performance by integrating acoustic and proprioceptive information through unknown mechanism/s. Two main types of local circuit neurons reside within the GCS: an inhibitory cell class similar to the cerebellar Golgi cells (Mugnaini, 1985; Ferragamo et al., 1998; Alibardi, 2002; Ryugo et al., 2003; Irie et al., 2006) and a cell class similar to the excitatory cerebellar unipolar brush cell (UBC) (Mugnaini et al., 1997; Slater et al., 1999; Diño et al., 2000a,b; Nunzi et al., 2000; Ryugo et al., 2003; Kalinichenko and Okhotin, 2005; Ito, 2006). While differences between Golgi cells and UBCs remained unclear for some time (Palay and Chan-Palay, 1974; Altman and Bayer, 1977; Mugnaini et al., 1980a), their separate identity was later firmly established in the cerebellum and the DCN of several mammalian species including primates (Mugnaini and Floris, 1994; Mugnaini et al., 1994; Rossi et al., 1995; Yan and Garey, 1998; Diño et al. 1999; Spatz, 1999; [2000]; [2001]; Ryugo et al., 2003; Alibardi, 2004; Sekerková et al., 2004b, [2005]; Simpson et al., 2005; Víg et al., 2005; Dugué et al., 2005; Crook et al., 2006; Rodrigo et al., 2006; Diana et al., 2007; Russo et al., 2007).

It is well established that neuronal systems performing similar computational tasks - e.g. the main and accessory olfactory bulbs, and the different spinal cord segments - contain similar microcircuits (Shepherd, 2004). A series of detailed studies using morphological and immunocytochemical methods (Mugnaini et al., 1980a,b; Wouterlood and Mugnaini, 1984;

Wouterlood et al., 1984; Blackstad et al., 1984; Mugnaini and Morgan, 1987; Berrebi and Mugnaini, 1988, [1991], 1993; Berrebi et al., 1990; Floris et al., 1994; Dunn et al., 1996) provided initial evidence that synaptic relations within the mammalian DCN are analogous to those of the cerebellar cortex, albeit with significant transformations, such as the absence of climbing fibers, an aspect also shared by piscine cerebellum-like structures (Mugnaini and Maler, 1993; Montgomery et al., 1985; Bell, 2001, 2002; Campbell et al., 2007). It has also been argued that the DCN pyramidal neurons might be analogous to the cerebellar eurydendroid cells of fishes, which in turn have been equated to mammalian cerebellar nuclei neurons drawn into the cortex. Subsequent electrophysiological and neurochemical investigations in several laboratories specified the similarities and the differences between CN and cerebellar neurons, expanding the view that the CN contains a cerebellum-like microcircuit without the climbing fiber component (Campos et al., 2001; Devor, 2000, 2002; Young and Oertel, 2004; Oertel and Young, 2004; Shore and Zhou, 2006; Tzounopoulos et al., 2004, 2007); this idea has now gained wide acceptance.

While many studies have been conducted on cerebellar UBCs, little is know about the UBCs that populate the CN. In the cerebellum, UBCs are strikingly enriched in regions receiving vestibular, spinal and trigeminal inputs, while they are rare or absent in areas densely innervated by the pontine nuclei (Diño et al., 1999). In the cerebellum of mouse, rat and monkey, two UBC subsets – primarily distinguished by expression of either the calcium binding protein calretinin (CR) or the metabotropic glutamate receptor mGluR1α (Nunzi et al. 2002, 2003; Sekerková et al., 2004b; Ilijic et al., 2005; Nunzi et al., 2006) - have distinct, but overlapping, distributions; and recent studies in the rat cerebellum have shown that the epidermal growth factor substrate 8 (Eps8) is densely expressed in both UBC subsets, while it is present at lower density in granule cells (Sekerková et al., 2007).

Although CR-positive (CR^+) and mGluR1α-positive ($mGluR1\alpha^+$) UBCs have been noted in the rodent CN (Floris et al., 1994; Wright et al., 1996; Jaarsma et al., 1998), no detailed map of UBCs in the CN exists, and it is still not known whether CR and mGluR1α in the CN are expressed in the same UBC, or whether these neurons co-distribute with granules in the entire GCS.

Here we used a specific monoclonal antibody to Eps8, alone or in combination with polyclonal antisera to CR and mGluR1α, to produce a congruent map of CN UBCs. Furthermore, the distribution of UBCs immunostained by antibodies to Eps8, CR and mGluR1α was verified with an antiserum to Tbr2, a transcription factor that is expressed by UBCs at early stages of development and continues to be expressed in the adult, albeit at lower level (Englund et al., 2006). The UBC map was then compared with that of granule cells labeled by the α6 subunit of the $GABA_A$ receptor, a protein transcribed in just two cell types: the cerebellar granule cells and the lineage-related cochlear nucleus granule cells (Kato, 1990; Varecka et al., 1994; Campos et al., 2001).

EXPERIMENTAL PROCEDURES

Animals

Sprague-Dawley rats were purchased from a commercial breeder and processed according to approved guidelines. All experiments conformed to protocols approved by the Northwestern University Animal Care and Use Committee. We followed guidelines issued by the National Institutes of Health and the Society for Neuroscience to minimize the number of animals used and their suffering.

Antisera and reagents

The sources of antisera and reagents were as follows: rabbit anti-Tbr2, rabbit anti-α6 subunit of the $GABA_A$ receptor, and mouse monoclonal anti-calretinin (Chemicon, Temecula, CA); mouse anti-Eps8 (BD Biosciences, San José, CA); rabbit anti-CR (SWANT, Bellinzona, Switzerland); rabbit anti-mGluR1α polyclonal antiserum (produced, characterized and given to us by Dr. R. Shigemoto, Myodaiji, Okazaki, Japan); biotinylated anti-rabbit and anti-mouse secondary antibodies (Amersham, Piscataway, NJ); Alexa-tagged anti-mouse and anti-rabbit antibodies (Molecular Probes, Eugene, OR); Vectastain Elite ABC and SG® peroxidase substrate kits and Vectashield mounting medium (Vector Laboratories, Burlingame, CA); all other chemical reagents (Sigma Aldrich, St. Louis, MO).

Fixation and tissue preparation

Twelve adult and six 28-day old rats (N=14) were deeply anesthetized with intraperitoneal sodium pentobarbital (60mg/kg body weight) and perfused through the ascending aorta with saline followed by 4% freshly depolymerized paraformaldehyde in 0.1 M phosphate buffer (PB), pH 7.4. After perfusion, brains were maintained *in situ* at room temperature for 1 hour, dissected, and then cryoprotected in 30% sucrose dissolved in phosphate buffered saline (PBS) at 4°C. Serial sections, 20–30μm thick, were cut in the sagittal, coronal and horizontal planes on a freezing stage microtome and collected in six sequential bins for immunostaining and standard Nissl staining.

Immunofluorescence

For immunofluorescence, sections were blocked with 3% NGS/1%BSA/TBS-T followed by incubation with the primary antibodies: mouse anti-Eps8 (1:1000); mouse anti-calretinin (1:2500); rabbit anti-mGluR1α (1:1000); rabbit anti-Tbr2 (1:1000), rabbit anti-calretinin (1:10000) and rabbit anti-α6 (1:1000). Bound primary antibodies were visualized by secondary antibodies coupled to Alexa 488 or Alexa 568 (Molecular Probes, Eugene, OR). Sections were mounted with Vectashield (Vector). For all experiments, control sections incubated without the appropriate primary antibody lacked immunoreaction signal. All single-labeled, double-labeled, and silver-intensified sections sections processed for brightfield microscopy were mounted on gelatin-coated slides, dehydrated, and coverslipped.

Immunohistochemistry

Antigen retrieval—To reduce background and enhance staining for Tbr2 and the α6 subunit of the $GABA_A$ receptor, free-floating sections were treated with 1% H_2O_2 and 10% methanol for 30 minutes in Tris buffered saline (TBS; 100 mM Tris, 150 mM NaCl; pH 7.4), incubated in a blocking solution containing 3% normal goat serum (NGS) and 1% bovine serum albumin (BSA) in TBS with 0.2% Triton X-100 (TBS-T) and subjected to antigen retrieval treatment. After mounting onto VWR® Superfrost® Plus Micro Slide and drying at 50 °C, sections were rinsed in PBS, and then autoclaved in 0.01M sodium citrate (pH 6.0) for 20 minutes at 121 ° C. After cooling, sections were rinsed and processed for single-label or double-label immunohistochemistry as described below.

Single-antigen labeling—Sections were processed for single-label immunohistochemistry with the Vectastain avidin/biotin peroxidase protocol. Briefly, using a 1% NGS/1% BSA/TBS-T diluent, primary antibody solutions containing either one of the following specific antibodies were prepared: Eps8 (diluted 1:2000), Trb2 (1:1000), mGluR1α (1:500), mouse anti-CR (1:3000), rabbit anti-CR (1:10000), or the α6 subunit of the $GABA_A$ receptor (1:1000). Sections were then blocked as described above and incubated in one of the primary antibody solutions for 36–48 hours at 4°C, rinsed several times in TBS-T and then incubated for 2 hours at RT with the appropriate biotinylated secondary antibody, diluted 1:500 in 1% NGS/1% BSA/TBS-

T. After rinsing in TBS, sections were incubated for 1 hour at RT with avidin/biotin using ABC Elite kit rinsed again and then and visualized using 0.05% 3,3- diaminobenzidine-HCL (DAB) and 0.01% H_20_2.

Double-antigen labeling—For two-color brightfield microscopy, free-floating sections immunoreacted for the first antibody reaction as indicated above were rinsed several times and incubated in a second primary antibody solution at 4°C for 24–48 hours, rinsed, and then treated with a solution containing the appropriate biotinylated species-specific secondary antibody (diluted 1:500) for 2 hours at RT. After rinsing, incubating in ABC elite solution, and then rinsing again, the peroxidase reaction was visualized using the Vector SG® peroxidase substrate kit.

Silver intensification of the peroxidase-DAB reaction—Silver intensification of single-labeled free-floating sections was done according to the procedure described by Quinn and Graybiel (1996). Briefly, free floating sections, processed using the DAB substrate, were rinsed three times in water, warmed in a 56–60 °C oven and then incubated for 10–12 minutes in a 0.5% ammoniacal silver nitrate solution. Following short rinses in water and 1% sodium thiosulfate, the sections were toned for 2 minutes in 0.2% gold chloride, rinsed, treated with 0.5% oxalic acid for 2 minutes, rinsed again and then treated for 5 minutes with 5% sodium thiosulfate.

Microscopy and photography

Brightfield and immunofluorescence images of brain stem sections were acquired with a Spot RT CCD video camera (Diagnostic Instruments, Sterling heights, MI, USA) mounted on a Nikon Eclipse E800 microscope. Laser scanning confocal images were obtained with a Nikon PCM 2000 Confocal Microscope System (New York, NY, USA), mounted on the Eclipse microscope. Images were analyzed individual or in z-stacks of different depths. For colocalization experiments type DF immersion oil (Fryer, Huntley, IL, USA) was used with either a 40X plan-fluor lens (numerical aperture 1.3) or a 60X plan-apochromatic lens (numerical aperture 1.4). To minimize spillover between the channels the images were sequentially acquired and saved as tiff files with150 pixels/inch resolution. All images were processed with Adobe Photoshop to adjust brightness/contrast without any other editing.

RESULTS

Cytoarchitecture of the CN

The cytoarchitecture of the rat CN is graphically represented in Fig. 1. Auditory nerve fibers have been schematically drawn in the sagittal section (Fig. 1D) to illustrate the fact that their ascending and descending branches respectively innervate anterior (AVCN) and posterior (PVCN) divisions of the VCN, both of which have a predominantly magnocellular cytoarchitecture; by contrast, the arching, descending branches innervate the polymorphic layer of the DCN. In the VCN, the auditory nerve root demarcates the border of AVCN and PVCN.

The rat CN contains a distributed system of granule cells (GCS) that is readily apparent in Nissl stained sections (data not shown), as previously described (Mugnaini et al., 1980a,b). CN regions that are enriched with granule cells are indicated using the terminology listed below, which corresponds to that adopted in most studies of the mammalian CN (with the exception that we added the *rostrodorsal lip* of the subpeduncular corner (see below). (1) The *lamina* is located at the border between VCN and DCN; (2) the *superficial granular layer (sgl)* forms a discreet sheet covering most of the VCN's pial surface; (3) the *clusters of DCN granule cells* are mostly situated in layer 2 and are also present in the polymorphic layer, with minimal

involvement of the molecular layer; (4) the *subpeduncular corner (spc)* is located at the dorsal edge of the VCN beneath the inferior cerebellar peduncle, and has a *floccular lip* that extends laterally into the stem of the flocculus, a *rostrodorsal lip* that extends along the superior cerebellar peduncle, and a *dorsomedial lip* that extends in between the cerebellar peduncles and the spinal trigeminal tract; (5) the *medial sheet (ms)* runs along the medial border of the VCN; (6) the *strial corner* forms the dorsomedial pole of the DCN above the dorsal acoustic stria; (7) the *granule cell islands* are scattered in the root of the VIIIth nerve. Furthermore, the *small cell cap (SCC)*, which is sandwiched between the superficial granular layer and the magnocellular portions of AVCN and PVCN, is a discontinuous skein of multipolar small cells that contains interspersed granule cells - although this region appears less distinct in rat than in other mammals (Osen, 1969; Moore et al., 1996), we prefer to use the term SCC instead of "small cell shell", by which some authors indicate the sum of SCC and SGL (Hurd et al., 2004). From these locations the thin granule cell axons reach the molecular layer of the DCN, where they form varicose parallel fibers synapsing with projection neurons and interneurons (Mugnaini et al., 1980b; Wouterlood and Mugnaini, 1984; Wouterlood et al., 1984).

UBC subclasses expressing calretinin and mGluR1α the CN

Initially, we set out to analyze UBCs in the CN with CR and mGluR1α antisera, as these have been very useful to identify UBCs in the cerebellum (Nunzi et al., 2002, 2003; Sekerková et al., 2004,2007). In cerebellar sections, CR immunoreaction highlights the somatodendritic compartment of one subset of UBCs and mGluR1α immunoreaction intensely labels the brush of a second UBC subset. Although subpopulations of mossy fibers and inhibitory granular layer interneurons also express CR and Purkinje cells and their dendrites are mGluR1α, these additional immunoreactivities do not interfere with UBC identification in the cerebellum.

Unlike the cerebellum, however, concomitant intense staining of other CR^+ and $mGluR1\alpha^+$ cellular elements in the CN made it cumbersome to clearly visualize UBCs (panels A–D of Fig. 2). Primary cochlear fibers and many types of neurons are CR^+, and fiber networks and different types of neurons, including cartwheel, pyramidal, and giant cells, are $mGluR1\alpha^+$ as described elsewhere (Arai et al., 1991;Rogers and Résibois, 1992;Lohman and Friauf, 1996;Wright et al., 1996; Petralia et al., 1996; Bilak and Morest, 1998;Korada and Schwarzt, 2000;Pór et al., 2005). CR^+ UBCs, therefore, could only be identified when their cell body, dendritic stem and brush all lay within the plane of the section (arrows in panels A–D of Fig. 2). Similarly, intensely $mGluR1\alpha^+$ (middle panels of rows A–D of Fig. 2) neuropil structures could be identified as UBC brushes, because they were sometimes observed in connection to their stem dendrites and parent cell bodies; this required high power lenses and was only possible in optimally stained sections (Figs. 3C F G and H, and 5 F J and K).

Nevertheless, using double-labeling and laser scanning confocal immunofluorescence microscopy we determined that UBCs expressing either CR or mGluR1α were present in every region of the GCS, albeit at varying densities (DCN, Fig. 2A; superficial granular layer, Fig. 2B; lamina, Fig. 2C; subpeduncular corner, Fig. 2D).

Two-color confocal microscopy also uncovered a complex situation that is partly different from that observed in the cerebellum: while the majority of UBCs in the CN expressed either mGluR1α or CR (Figs. 3E and F), some of them were double-labeled (Fig. 3G, 5J and K). These double-labeled cells represented a small minority, perhaps less than 10%, still to be precisely assessed with quantitative methods; they were spotted more frequently among fiber bundles at the borders of the CN and in the SGL than in other CN regions.

Eps8 and Tbr2 cell-class markers for UBCs

To more readily identify CN UBCs, we then turned to antisera against the actin-binding protein Eps8 and the transcription factor Tbr2 (Fig. 3 and 4), both of which stain fewer cellular elements than CR and mGluR1α (Englund et al., 2006;Sekerková et al., 2007). In the cerebellum of adult rats, Eps8 is expressed intensely in UBCs and weakly in granule cells (Offenhauser et. al., 2006;Sekerková et al., 2007); and immunostaining for Tbr2 is present primarily in the UBC nuclei (Englund et al., 2006; and our Fig. 4G) - although a very weak segnal also occurs in the nuclei of molecular layer granules that have failed to migrate into the granular layer (data not shown). Likewise, in the CN of adult rats Tbr2 labeling is confined to the nuclei of UBCs (Fig. 3H–J, 4H and 5G).

Dual-label immunofluorescence and laser scanning confocal microscopy were used to assess which of the two main UBC subsets in the CN share the Eps8 epitope. Out of fifty mGluR1α-expressing and fifty CR-expressing UBCs selected at random from different regions of the CN, all were $Eps8^{+}$. Individual representative cells are shown in Fig. 3A and 3C. In analogy with the cerebellar cortex, all regions of the CN additionally contained substantial proportions of $Eps8^{+}/CR^{33}$ UBCs (Fig. 3B) and $Eps8^{+}/mGluR1\alpha^{-}$ UBCs (Figs. 3D). The data indicated that Eps8 epitope colocalized with both CR and mGluR1α in most if not all UBCs and, therefore, is a valid UBC population marker.

To determine whether Tbr2, like Eps8, is a population marker for CR and mGluR1α UBC subclasses in the CN, sections were stained with Tbr2/CR and Tbr2/mGluR1α antibody pairs (Fig. 4). Because antisera to Tbr2 and mGluR1α are both rabbit polyclonals, we used sequential two-color immunoreactions and brightfield immunocytochemistry. As for Eps8, fifty randomly chosen CR-expressing UBCs from different CN regions were $Tbr2^{+}$ and another fifty mGluR1α-expressing UBCs were $Tbr2^{+}$. As shown in Fig. 3H–J, the corresponding individual sections contained not only $Tbr2^{+}/mGluR1\alpha^{+}$ or $Trb2^{+}/CR^{+}$ UBC (red and black asterisks), but also $Tbr2^{+}/mgluR1\alpha^{-}$ or $Tbr2^{+}/CR^{-}$ UBCs (white asterisk).

The map of UBCs in the CN

Immunostaining with antibodies against the two cell population markers, Eps8 and Tbr2 applied either individually or -more effectively-together, turned out to be a superior means to map UBCs at low magnification in brightfield microscopy (Fig. 4). Panel A–B of Fig. 4 serve to compare the patterns of immunostaining in lobule VII *vs.* lobule X of the cerebellar vermis known to contain low and high densities of UBCs, respectively, while panels C–F show the different densities of UBCs in different regions of the CN. The high density of UBCs in layer 2 and the polymorph layer of the DCN (Fig. 4D) paralleled that in lobule X. UBCs also occurred at high density in portions of the main body of the subpeduncular corner (not shown, but see Figs. 2D and 6F), and at moderate densities in all other regions of the GCS - including the medial sheet (Fig. 4C), the superficial granular layer (Fig. 4C and F) and the lips of the subpeduncular corner (data not shown) - with the exception of the lamina, in which they occurred only rarely (Fig. 4E). The vestibular nerve root (Suppl. Fig. 1D) and parts of the magnocellular regions of the VCN, particularly the rostrodorsal portions of AVCN and PVCN (Figs. 4C and 6G) also contained UBCs identified by Eps8 and/or Tbr2 immunoreactivity.

The varying densities of UBCs in regions of the CN were also readily apparent in sections immunostained with Eps8 antiserum using a DAB protocol followed by silver intensification (Suppl. Fig. 1). Silver intensification contrasted the substantial intermingling of UBCs with the spherical bushy cells in the AVCN against the very sparse UBC population of the ventral PVCN, as best appreciated in horizontal sections (Suppl. Fig. 1B and C). The various staining protocols corroborated the notion that at high antisera dilution (⟩1:3000) the UBCs are the only intensely $Eps8^{+}$ neuronal cells in both cerebellar cortex and CN (deep blue stain in Fig. 4,

panels A–D); granule cells were immunostained, but barely above background, while their parallel fiber axons were moderately Eps8$^+$ in the molecular layer of both cerebellum (labeled ml in Fig. 4, panels A and B) and CN (layer 1 in Fig. 4D). We also saw Eps8$^+$ small axon terminals of presumed extrinsic origin/s in the cerebellar nuclei (data not shown) and the CN (Fig. 4, bottom of panel C), but this is outside the scope of the present study.

Taken together, the data are compatible with the notion that Eps8 and Tbr2 antisera provide largely similar immunostaining patterns in the cerebellum and the CN and are reliable markers for UBCs, particularly when used with double labeling protocols.

Ectopic UBCs

UBC-like cells were also found in areas that are situated outside the widely accepted CN borders and included the trapezoid body, the trigeminal tract, the spinal and principal trigeminal sensory nuclei, the cerebellar peduncles, the vestibular nuclei and the pedunculopontine region. These cells, which we interpreted as"ectopic" UBCs on the basis of their distinctive immunostaining by Eps8 (with or without silver intesification) and Tbr2, or by combined Eps8/Tbr2 labeling, will be considered further in a separate section dedicated to re-consideration of the CN granule cell domain (see below).

Diversity of morphological phenotypes of CN UBCs

Throughout the CN, the UBCs showed a range of morphological variations (Figs. 4 and 5). In the majority of UBCs, the dendrite measured 5–20 μm in length and its stem terminated with a brush 8–10 μm long and 7–12 μm wide. The dendrite had a straight course (Fig. 5B) or was curved (Fig. 3E), sharply bent (Fig. 5E) or twisted (Fig. 5J). Other UBCs had a brush at the end of a stunted dendrite (Fig. 5A and K) or they lacked a dendritic stem altogether, but had a brush or multiple dendrioles arising directly from the cell body (Fig. 5A and H). A rare UBC had a dendrite dividing in two branches each provided with a brush (Fig. 5I); and pairs of UBCs whose brushes occupied the same glomerulus were also encountered (Fig. 5C and L; see also Ryugo et al., 2003). Many of the UBCs whose cell bodies were situated between nerve fiber bundles emitted a dendrite that exceeded the usual length and measured up to 35–50 μm (Fig. 5J); and in the DCN molecular layer we observed UBCs whose dendrite showed a long, curved dendrite ending with a brush in the pyramidal cell layer (data not illustrated). Overall, the most unusual forms of UBCs were encountered in regions known to contain rare granule cells. Many of the UBCs situated in the superficial granular layer and the DCN showed thick, globular brushes presumably made up of many dendrioles (Fig. 3A, D and E), while the large majority of UBCs situated in the auditory and vestibular nerve roots, the medial sheet and the subpeduncular corner were provided with thinner and elongated (4 μm × 20 μm) or irregularly shaped brushes, likely consisting of fewer and/or longer dendrioles (Figs. 3C, F; 5G and J). Occasionally, the brushes had a particularly dense appearance (Figs. 3F and 5K) and some of them belonged to UBCs that expressed both CR and mGluR1α also in their perikarya (Fig. 5K).

In general, when compared to those in the neighboring granular layer of the cerebellar flocculus, UBC brushes in the CN appeared less uniform and their stem dendrites could be followed less frequently to the parent cell body because of their tortuous course. Nevertheless, the phenotypic variation of the UBCs ranged similarly in the two hindbrain regions.

Laser scanning confocal immunofluorescence microscopy of the brushes of CN UBCs also revealed Eps8 enriched postsynaptic foci that varied considerably in shape and size in (Figs. 3–5) Similar Eps8 “hotspots” have been shown previously to be in register with the actin-rich postsynaptic apparatus of cerebellar UBCs (Sekerková et al., 2007). Because dense CR immunostaining of the cytosol obfuscated details of postsynaptic specializations in CR$^+$ UBCs,

these Eps8-enriched foci were more readily visualized in Eps8/mGluR1α (Fig. 5F) and Eps8/Tbr2 immunostained sections (Fig. 4H). The Eps8-enriched foci appeared either as large entities (elongated or ring-like structures in Figs. 3C, 5D and F), or as multiple small, variously fragmented patches (Figs. 4H, 5A–B and E). UBCs from each of the different CN regions contained one or the other, or even both, the main forms of Eps8 foci.

The granule cell domain of the CN revisited in relation to UBCs

Because cochlear granules are difficult to identify unequivocally when they occur at low density in the tissue (Mugnaini et al., 1980b), we took advantage of the fact expression of the $GABA_A$ α6 subunit is restricted to granule cells of both cerebellum and cochlear nucleus (Kato, 1990; Laurie et al., 1992; Varecka et al., 1994; Bahn et al., 1997; Campos et al., 2001), to produce a detailed map of α6-stained granule cells in the CN and to revisit the GCS of the CN (Suppl. Fig. 2).

To ascertain whether ectopic UBCs occurred in combination to granule cells and evaluate the relative densities of granule cells and UBCs, we first double labeled sections with antisera to α6, as a marker for granule cells, and to Eps8, as a marker for UBCs, and established that UBCs are α6-immunonegative (Fig. 6A and B).

After antigen retrieval, which turned out necessary for robust immunostaining, α6 antiserum intensely stained the tips of granule cell dendrites in the glomeruli of the cerebellum (Fig. 6B) and the CN (Suppl. Fig. 2B); it also delicately outlined the plasmamembrane of the granule cell bodies (Figs. 6B and Suppl. Fig. 2), thus revealing both postsynaptic and extrasynaptic membrane regions as reported (Nusser et al., 1996). As expected, we observed granule cells in all the regions of the CN previously attributed to the GCS (Fig. 6 and Suppl. Fig. 2). The highest densities of granule cells were present in the lamina and superficial granular layer, followed by layer 2 and polymorphic layer of the DCN and the subpeduncular corner, with lower densities in the medial sheet the strial corner and the cochlear nerve root. Additionally, we observed $\alpha6^+$, "ectopic" granular neurons scattered in the magnocellular regions of the VCN, especially the rostrodorsal portions of the AVCN and PVCN (Figs. 6E–G and Suppl. Fig. 2), the vestibular nerve root (not shown), the lateral part of the ventral acoustic stria (or trapezoid body) (Fig. 6E), the spinal trigeminal tract and the spinal and principal trigeminal nucleus (Suppl. Fig. 2A and E), the inferior and medial cerebellar peduncles (Suppl. Fig. 2D and E), the ventral spinocerebellar tract (Suppl. Fig. 2A), the vestibular nuclei and the Y and X nuclei (not shown). In some of the sections, strings of granule cells provided continuity between these regions and the granules cells of the medial sheet, the lips of the subpeduncular corner and the strial corner (Suppl. Fig. 2A, D and E).

We then turned to double-immunostaining with antisera to Tbr2 and α6, which provide contrasting staining of cellular nucleus and somatodendritic plasmamembrane, respectively. Dual-labeling faithfully reproduced the densities of granule cells and UBCs observed after individual immnostaining. UBCs accompanied granule cells in both the established subregions of the GCS and the "ectopic sites" (Fig. 6). Furthermore, we firmly established that the DCN has the highest ratio of UBC/granule cells and the lamina the lowest (compare panels D and G of Fig. 6). Given the restricted expression of the α6 subunit and Tbr2, we presumed that the $\alpha6^+$cells and the $Trb2^+$ cells outside the established GCS are indeed "ectopic" granules and UBCs. Immunostaining also suggests that ectopic $\alpha6^+$ granules possess dendrites that differ from those of canonical granules, in so far as they are longer and more often branched and are provided with short appendages that bear some resemblance to spines (Suppl. Fig. 2B and C). Thus, the variabilities of dendritic configurations in CN granule cells and UBCs may be in register.

DISCUSSION

This immunocytochemical study establishes the UBCs as a major neuronal cell class in the primary auditory center of the rat brainstem, explores the degrees of chemical and morphological similarities between CN and cerebellar UBCs, provides the first congruent map of CN UBCs, and highlights their uneven density in the nuclear subdivisions. Furthermore, the study demonstrates that CN UBCs accompany granule cells, albeit with varying ratios, and provides a more accurate map of CN granule cells than previously obtained. The morphological and chemical phenotypes of CN UBCs were analyzed using antisera to four different cell markers previously shown to label UBCs in the cerebellar cortex: Eps8 Tbr2 mGluR1α and CR (Nunzi et al., 2002; Englund, 2006; Sekerková et al., 2007), and the topographic relations between UBCs and granule cells were established by double-labeling with Trb2 and the α6 subunit of the $GABA_A$ receptor.

Chemical phenotypes of UBCs in the CN

Our data demonstrate that the transcription factor Tbr2 and the actin-binding protein Eps8, which have complementary nuclear and cytoplasmic localizations, are valid markers for the UBC population of the rat CN. Expression of Tbr2 can already be detected in both granule cell and UBCs lineages at early developmental stages (Englund et al., 2006), but is maintained in adult rats in the UBC population; on the other hand, expression of Eps8 accompanies maturation of postsynaptic specializations in both granule cells and UBCs (Diño and Mugnaini, unpublished observations), and is conveniently much stronger in the latter (Sekerková et al., 2007; and the present study). Although it is still not proven that every mature UBC expresses both Eps8 and Trb2, our study provides the first demonstration that the majority, if not all, of the $Eps8^+$ or $Tbr2^+$ cells are either $CR^+/mGluR1\alpha^-$ or $mGluR1\alpha^+/CR^-$, indicating that CN UBCs display heterogeneous chemical phenotypes as do cerebellar UBCs in mouse (Nunzi et al., 2002), rat (Sekerková et al., 2004), and Rhesus monkey (Nunzi et al., 2006). Furthermore, evidence from laser scanning confocal immunofluorescence microscopy indicates that a small proportion of CN UBCs display both CR and mGluR1α immunoreactivities, an observation that is in sharp contrast to the separation of the CR and mGluR1α phenotypes in the vestibulocerebellum of adult mice and rats (Nunzi et al., 2002; Sekerková et al., 2004).

Developmental studies also point to differences between the two UBC populations. Recently, knowledge concerning the axial origins and lineage and sublineage relationships of the component neurons and afferent pathways in cerebellum and CN has been augmented by novel molecular strategies (Fünfschilling and Reichardt, 2002; Zervas et al., 2004; Machold and Fishell, 2005; Wang et al., 2005; Englund et al., 2006; Farago et al., 2006; Hoshino, 2006; Joyner and Zervas, 2006; Morales and Hatten, 2006; Howell et al., 2007; Pasqualetti et al., 2007; Salero and Hatten, 2007). There is now agreement that the cerebellum derives from the rhombomere 1 territory of the rostral (or anterior) rhombic lip, while the cochlear nuclei may derive from the rhombomeres 2–5 territory of the caudal (or posterior) rhombic lip and adjacent dorsal neuroepithelium (Ivanova and Yuasa, 1998; Farago et al., 2006; Morales and Hatten, 2006; Saul et al., 2007). A model generated by intersectional and subtractive genetic fate maps suggests that large neurons of the AVCN arise from progenitors in rhombomeres 2–3, those of the PVCN from rhombomere 4, and DCN neurons from rhombomeres 4–5 (Farago et al., 2006). On the other hand, authors agree that cerebellar granule cells and CN granule cells originate from contiguous precursors pools in the rostral and caudal rhombic lip (Machold and Fishell, 2005; Wang et al., 2005; Englund et al., 2006; Farago et al., 2006; Morales and Hatten, 2006), the rhombomere 1 for cerebellar granules and the rhombomeres 2–5 for CN granules (Farago et al., 2006). As Englund et al. (2006) indicated that cerebellar UBCs also arise from the rostral rhombic lip as do cerebellar granules, co-distribution of UBCs and granule cells in the CN may suggest that the CN UBCs also arise from rhombomeres 2–5. Neurons providing

many of the fiber systems innervating cerebellum and cochlear nuclei also derive from the rhombic lip region, but the specific points of origin of the precursors are debated (Zervas et al., 2004; Machold and Fishell, 2005; Wang et al., 2005; Englund et al., 2006; Farago et al., 2006; Morales and Hatten, 2006). The “ectopic“ UBCs described in the present study presumably mark the developmental routes of the fiber pathways projecting to the CN.

The presence of three sets of UBCs in the CN re-emphasizes the need to discover the factors that determine sublineage differentiation within this highly specialized cell population. Given the apparent generality of Tbr2 expression in the UBC population, are the different UBC subsets determined by additional transcription factors acting on a single pool of committed precursors, by topographic or time-dependent differences in the proliferative matrix, or epigenetically by the afferents/target relations established early during development? The possible involvement of differential time-related factors is supported by the study of Sekerková et al., (2004b), which showed that the peak times of prenatal production of the two cerebellar UBCs subsets in the rat are slightly different and both occur after generation of Purkinje cells and cerebellar nuclei neurons; however, analogous information on CN UBCs is lacking.

Morphological phenotypes of UBCs in the CN

We found that the morphological phenotype of UBCs in the CN shows notable variations. The range of forms in the CN is similar to that in the cerebellum, while the proportion of unusually shaped UBCs is higher in CN. Variations in cell shape in the CN appeared to be related to variations in cellular and fiber densities; indeed, many UBCs present a typical shape in the superficial granular layer and the DCN, both of which are regions of high cellular density, while variant forms occur frequently in the VCN, the medial sheet and the eight nerve roots, i.e, regions with an abundance of nerve fibers. Some of these variants resemble neurons described by others as shrub cells (Brawer et al., 1974), mitt cells (Hutson and Morest, 1996; Hurd et al., 1999; Josephson and Morest, 2003), and chestnut cells (Weedman et al., 1996; Alibardi, 2004, 2006). It is possible that such neurons are, in fact, forms of UBCs, rather than specific cell classes as it has been proposed elsewhere. Direct proof of this tentative interpretation will obviously require detailed light and electron microscopic analysis of a large sample of variant cell forms using appropriate combinations of cell markers and tract-tracing methods.

Distribution of UBCs and granule cells in the CN

The congruent maps of CR-expressing and mGluR1α-expressing UBCs demonstrate that the two UBC subsets have overlapping distributions in the CN. In the absence of precise differential cell counts for the two major UBC subsets, there are three findings concerning the map of CN UBCs that appear most noteworthy, namely: a) the high density of UBCs in the DCN and subpeduncular corner; b) the extremely low density of UBCs in the lamina, compared to other regions of the GCS; and c) the presence of UBCs in magnocellular parts of the VCN and in territories contiguous with the CN.

Because the cerebellar UBCs lie nearly exclusively within the granular layer at varying UBC/granule cell ratios among the different lobules, we expected in the CN UBCs would likewise co-distribute with granule cells at varying UBC/granule cell ratios across the different regions of the GCS. Yet, the high densities of UBCs in layer 2 and deep region of the DCN and the subpeduncular corner were a remarkable finding, as they closely approached UBC densities in the caudal cerebellum, which processes sensory signals concerning the head position in space and regulates vestibulo-ocular reflexes (Diño et al., 2001; Sekerková et al., 2005). As indicated for the DCN and the lamina, strikingly diverse granule cell/UBC ratios exist across the GCS. Furthermore, the rarity of UBCs in the lamina, with its compact cellular structure and well-known density of granule cells, requires a hypothesis, if not an explanation. Could it be that

mossy fibers innervating the lamina are repulsive to UBCs? In support of this hypothesis there are several observations of repulsive effects during development of the cerebellar system (de Diego et al., 2002). Moreover, a study on the distribution of cerebellar UBCs in different mammals had shown that these neurons occur only rarely in regions of the granular layer that are densely innervated by mossy fiber terminals of the basilar pontine afferents, even where these regions abut portions of the granular layer that are enriched with UBCs, as in the flocculus/paraflocculus complex (Diño et al., 1999). We found it interesting, therefore, that UBCs are most numerous in the DCN, which is the part of the CN that does not receive pontine afferents (Ohlrogge et al., 2001); and pontine afferents, instead, form clusters in other regions of the GCS including the subpeduncular corner (Ohlrogge et al., 2001), which also has areas with high and low densities of UBCs (Figs. 1D and 6F).

At the outset of our analysis, insufficient knowledge about the extent of distribution of granule cells hampered an explanation of the occurrence of UBCs in the VCN and the vestibular nerve root, as well as in other territories contiguous with the CN. These UBCs were denoted as "ectopic" to separate them from those in established subregions of the GCS. As previously reported, the nucleus of CN granule cells is less distinctly spherical and lighter than that of cerebellar granules, it often has a deep indentation, and may be easily confused with that of astrocytes even in well stained Nissl sections (Mugnaini et al., 1980b). It was therefore necessary to specifically label CN granule cells with a *bona fide* cell population marker. We confirmed that granule cells distributed throughout the CN's GCS express the rare $GABA_A$ α6 subunit, as do cerebellar granules, and utilized this marker in combination with Tbr2 as a non-interfering stainer of the UBC nucleus. It should be recalled that in spite of the shared expression of α6, as well as other markers such as of the zinc finger protein *zic* (Aruga et al., 1994), and certain electrical signatures (Rusznak et al., 1997), CN granules differ from cerebellar granules in other respects: their dendrites do not always form typical digitiform claws at their tips, a properties that they seem to express only when they cluster at high density; they lack the $GABA_A$ δ subunit, which is thought to confer onto neurons the property of tonic inhibition (Rossi and Hamann, 1998; Campos et al., et al., 2001; Wei et al., 2003; Peng et al., 2004; Balakrishnan and Trussel, 2007); they show a strong inhibitory response to glycine (Balakrishnan and Trussel, 2007) and have specific pharmacological properties (Boehm et al., 2006). Thus, it is understood that neither the UBCs nor the granule cells of the CN are identical to those in the cerebellar folia that have been studied so far.

Our maps demonstrate that both granule cells and UBCs regularly occur beyond the strict borders of the CN and that the GCS may be more extended than previously thought. Taken together, the data indicate that the maps of UBCs and granule cells produced by the present immunocytochemical investigation are likely to be in register. Because electrical activity plays an important role in neuronal proliferation, migration and differentiation (Spitzer, 2006), one may tentatively propose that afferent innervation influences the extension of granule cell and UBCs domains beyond the traditionally recognized domains. As considered below, this hypothesis is supported by data from the literature.

Mossy endings in the GCS

Studies from different laboratories over the last ten years have shown that the distributed GCS contains numerous complex synaptic fields, or glomeruli, consisting of pre- and post-synaptic neuronal processes surrounded by a wrap of astrocytic lamellae. These arrays are centered on a large axon terminal resembling a cerebellar mossy fiber rossette; this contains round synaptic vesicles and is surrounded by dendrites of granule cells and UBCs, which in turn are contacted by axonal boutons of intrinsic Golgi cell-like interneurons and perhaps also of other inhibitory neurons different from Golgi cells, that modulate the output of granule cells and UBCs. The fibers providing the central innervation of these neuropil arrays have been termed "cochlear

mossy fibers", because they form glomeruli similar to those in the cerebellar granular layer, albeit often smaller and/or less globose. Given that during cerebellar development the formation of full-fledged rosettes is attained only after convergence of a large number of granule cell and/or UBC dendrites in the glomerulus (Mugnaini and Forströnen, 1967; Altman and Bayer, 1996; Morin et al., 2001), the size difference of GCS and cerebellar glomeruli might be attributed to the relative densities of granule cells. The matter is further complicated by the termination in the CN's GCS of afferents that form not only large endings but also small endings of the en passant and terminal varieties. How does one define, therefore, the afferent systems in territories -like those pertaining to the GCS- that contain compact bands, clustered, or even scattered, granule cells and UBCs? Moreover, do allor only part of the GCS afferents target both granule cells and UBCs?

Several considerations engender considerable difficulties in classifying the GCS innervation and define its origins. First, while some of the fibers with small boutons may belong to branches of genuine mossy fibers that fail to develop typical rosettes or innervate a variety of neurons, others presumably belong to the - sometimes overlooked - modulatory aminergic and cholinergic pathways (Yao et al., 1996; Moore, 1988; Yao and Godfrey, 1999; Behrens et al., 2002) analogous to the non-laminar afferents innervating the cerebellar cortex (Voogd et al., 1996). Second, Morest and coworkers (Morest, 1997; Hutson and Morest, 1996; Hurd et al., 1999) have drawn attention to the presence of a different synaptic array in the CN neuropil, the "synaptic nest", which is unrelated to granule cells and may contain a large axon terminal. Third, $\alpha6^+$ granule cells situated outside clusters of like cells do not have typical dendritic claws, as shown in Fig. 6 and Suppl. Fig. 2C, and conceivably receive afferent boutons on their stem dendrites. Fourth, it may be difficult to establish the specific location of neurons giving rise to GCS afferents (Alibardi, 2003b), because of methodological pitfalls, such as labeling of fibers of passage, anterograde or retrograde filling of recurrent axon collaterals, transneuronal transport, and anectodal or equivocal images of degenerating neuronal profiles after long postlesion intervals (Kane, 1977). Fifth, the sample size of synaptic connectivity in several studies is limited, because reliable ultrastructural information requires labor-intensive analysis by serial section electron microscopy, which is severely hampered by time and cost considerations. Sixth, electron microscopic analysis of GCS afferents may be confounded by variations in their internal structure or questionable tissue preservation.

In their review on the neuronal microcircuits of the DCN, Dunn et al. (1996) subdivided the large, mossy terminals synapsing with granule cells in the guinea pig DCN into four main categories, on the basis of four variables of their internal structure: size and density of small clear synaptic vesicles, smallest mitochondrial diameter, and frequency of large dense core vesicles. Dunn et al. (1996) proposed that "the heterogeneity of mossy fiber rosettes in the CN indicates that they originate from different neuronal pools", based on observations that individual neuronal types are usually homogeneous with respect to their axonal organelles (Peters et al., 1991). Indeed, we now know that inputs to the GCS of CN originate from numerous auditory as well as non-auditory sources (Ryugo et al., 2003a,b; Alibardi, Zhan and Ryugo, 2007); while some of the inputs represent *bona fide* mossy fiber pathways, including auditory neurons still to be specified, lateral reticular nucleus, spinal trigeminal nucleus, pons nuclei, cuneate nucleus and cervical ganglion, others remain of uncertain nature, as considered below.

Sources and distribution of GCS afferents

The non-auditory projecting structures include: trigeminal and cervical dorsal root ganglia (Pfaller and Arvidsson, 1988; Shore et al., 2000; Zhan et al., 2006); spinal trigeminal nucleus (Itoh et al., 1987; Wolff and Kunzle, 1997; Li and Mizuno, 1997; Haenggeli et al., 2005; Shore, 2005; Shore and Zhou, 2006); cuneate nucleus (Itoh et al., 1987; Weinberg and Rustioni,

1987; Wright and Ryugo, 1996; Wolff and Kunzle, 1997; Shore and Zhou, 2006); basilar pontine nuclei (Ohlrogge et al., 2001); lateral reticular nucleus (Zhan and Ryugo, 2007); and primary and secondary vestibular fibers (Burian and Gstoettner, 1988; Kevetter and Perachio, 1989; Bukowska, 2002; Newlands and Perachio, 2003). GCS afferents from auditory centers include: collaterals of the cholinergic neurons (McDonald and Rasmussen, 1971; Vetter et al., 1993); the superior olivary complex (Kane 1977; Shore and Moore, 1998); inferior colliculus (Saldaña, 1993; Caicedo and Herbert, 1993; Malmierca et al., 1996; Alibardi, 2004); collaterals of DCN pyramidal cell axons (Smith and Rhode, 1985; Alibardi, 2004); and ipsilateral VCN and commissural CN neurons (Shore and Moore, 1998;Alibardi, 2004; 2006). And these lists might still be incomplete.

In an extensive series of studies, Alibardi (2004, 2006) circumvented some of the caveats of hodological neuroanatomy by making very large WGA-HRP injections in the ipsilateral AVCN, contralateral CN, and contralateral inferior colliculus and analyzing over three thousands mossy endings in the rat CN, even though this carried the risk of labeling axons of passage and recurrent collaterals of projection neurons. Although Alibardi mainly analyzed individual sections, he succeeded in identifying labeled mossy endings from *all three* sources that formed synaptic junctions with *both* granule cells and UBCs. Furthermore, while the majority of the labeled mossy endings contained round synaptic vesicles indicative of excitatory projections, he made the intriguing observation that a small percentage of the labeled mossy endings contained pleomorphic and/or flattened vesicles usually associated with GABA and/or glycine neurotransmission. The cerebellar counterpart of these inhibitory terminals would be the small percentage of mossy fibers originating from inhibitory projections neurons of the cerebellar nuclei (Batini et al., 1992; Mugnaini, 2000).

Another important issue is whether different afferent systems innervate the GCS in its entirety or are restricted to particular subregions. Light microscopic studies have shown that projections from cortex, sensory trigeminal nuclei and cuneate nucleus target the entire GCS, while other projections terminate in more restricted portions of the GCS. Remarkably, the pontine nuclei distribute largely over superficial granular layer, lamina, medial sheet and subpeduncular corner, but strikingly avoid the DCN, in partial contrast to the wider bouton-type termination of the direct pathway from the auditory cortex; this suggests a differential role for the cortico-nuclear and cortico-ponto-nuclear fibers. Direct afferents from the C2 spinal ganglion cluster mostly in the subpeduncular corner; and UBCs and granule cell islands in the auditory and vestibular nerve root are likely to receive afferents from restricted sources.

Studies in the cat have shown that the rostrodorsal portion of the VCN, that presumably correspond to the VCN region that in the rat contains UBCs and granule cells, receives many different types of non-cochlear afferents (Cant and Morest, 1978), one or more of which could be the source of mossy fibers targeting UBCs and granules interspersed among the bushy cells characterizing for this CN division; moreover, the ventral portion of the PVCN, which receives fewer non-cochlear projections, contains only rare UBCs. Osen et al. (1984) suggested that VCN granule cells are innervated by cholinergic afferents. The low density of UBCs in the SCC appeared roughly in register with the known presence of scattered granule cells in this narrow and non-distinct region of the rat VCN, which is also known to receive non-cochlear afferents (Mugnaini et al., 1980b; Osen et al., 1984). The occurrence of UBCs and granules in the auditory nerve root (see also Hutson and Morest, 1996) may also be in line with the observation of non-cochlear afferents among the primary auditory fibers and, similarly, their unexpected occurrence in the vestibular nerve root could be related to putative non-cochlear afferents that exist in kitten and were shown to pierce the vestibular nerve root (Cant and Morest, 1978). On the other hand, it is intriguing to speculate that UBCs and granules of the vestibular nerve root, in spite of their location, actually belong to the GCS of the CN and receive vestibular information that is transmitted to neurons of the DCN by granule cell axons. If so,

one should find labeled granule cells in the vestibular nerve root that are retrogradely labeled by tracer injection in the DCN. This hypothesis is compatible with the study of Zhao et al. (1995), who found presumptive granule and others small cells in the cat vestibular nerve root after tracer injections into “marginal shell regions” of the AVCN; it is likely that their tracer injections labeled granule cell axons coursing towards the DCN. Moreover, McCue and Guinan (1994), Burian and Gstoettner (1988) and Kevetter and Perachio (1989) described a vestibular saccular fiber in the cat that arborized in the ventromedial CN.

Granule cells and UBCs were also observed along fiber tracts known to carry somatosensory and descending afferent fibers to the CN, namely the ventral, intermediate and dorsal acoustic striae, the inferior and medial cerebellar peduncle and the spinal trigeminal tract, and also within the spinal trigeminal nucleus, the vestibular nuclei, and the cell groups of the vestibular region denoted Y and X. It should be noted that the subpeduncular corner is a region of high density of both granules and UBCs and forms a sizeable entity with its main body and extentions - the floccular lip, the dorsomedial lip, and the previously undescribed dorsorostral lip, that branch further along and into the medial cerebellar peduncle, the ventral spinocerebellar tract and the lateral pedunculopontine nucleus. It appears that the wider subpeduncular corner corresponds to the area termed “paracochlear glial substance” in the atlases of Paxinos and Watson (1998) and Paxinos et al. (1999) and, more appropriately, “ CNspr” (for Cochlear Nuclei, subpeduncular granular region) in the atlas of Swanson (1992). This wide territory contains various fiber systems, which may provide adequate inputs for ectopic CN and cerebellar neurons. Indeed, ectopic Purkinje cells, granule cells and UBCs that remain trapped in the white matter because of incomplete or faulty migration can nevertheless survive well into adulthood and form synaptic junctions (De Camilli et al., 1984; Ibrahim et al., 2000; Sekerková et al., 2004a; Ilijic et al., 2005). We found it notheworthy that in our α6/mGluR1α labeled section series Purkinje cells were rarely encountered in the subpeduncular corner and its extended lips (unpublished observations), which suggested that its granule cells and UBCs belong to the CN. Mapping the axonal projection/s of granules in the lips of the subpeduncular corner and/or their expression of the $GABA_A$ δ subunit may be necessary, however, to firmly establish to what extent cerebellar and cochlear granule cell systems are separate anatomical entities.

The questions of the termination in the GCS of fibers from the spiral ganglion and the auditory cortex are still open, in spite of repeated investigations. Remarkably, several studies indicate that primary cochlear afferents do not form synapses with granule cells (Merzenich et al., 1973; Rouiller et al., 1986; Malmierca, 2003) and UBCs in spite of their close spatial relations. This is in contrast to the vestibular system, which shows a dense, direct projection from the Scarpa’s ganglion to the granular layer of vermal lobules IX and X (Korte and Mugnaini, 1979; Barmack et al., 1993; Diño et al., 2001; Newlands and Perachio, 2003; Sekerková et al., 2005). Primary cochlear afferents, which are numerous, relatively thick and tonotopically arranged, densely innervate both the magnocellular portions of AVCN and PVCN and the small cell cap (Osen, 1970; Merchan et al., 1985, 1986). There is no report, so far, of an input to granule cells or UBCs from specifically labeled type I primary fibers (Fekete et al., 1984; Benson and Brown, 2004), even though the threshold for *c-fos* activation in granule cells is lower than that for other CN neurons (Yang et al., 2005). By contrast, there is some uncertainty about the targets of type II cochlear afferents, which are few and thin and project more diffusely than type I fibers. Type II fibers have *en passant* and terminal swellings, some of which are not synaptic, while others form synaptic junctions predominantly innervating stellate cells in the SCC and the lamina and large cells in the VCN. Scattered thin fibers labeled from the preriphery were seen by light microscopy meandering in the superficial granular layer and forming varisized varicosities along their course, with the largest approaching 8 μm in diameter (Shore and Moore, 1998). Two studies are in agreement that presumed type II fibers do not form synaptic junctions with granule cells, although they may have physical contact them

(Hurd et al., 1999; Benson and Brown, 2004). There is an isolated report of a single, small terminal of a type II fiber nested among small dendritic profiles, whose identification as granule cell dendrites is unconvincing (Berglund et al., 1996). In another report, putative type II fibers were seen in contact with “mitt cells” (probably a form of UBCs, see above) but without synaptic apposition (Hurd et al., 1999). Although the weight of the evidence is certainly that primary auditory fibers do not synapse with either granule cells or UBCs, further studies using dual-label protocols are warranted to increase the sample size of the boutons of type II fibers and their potential target cells.

There is agreement that the direct projection to the GCS from the auditory cortex to the GCS is excitatory, albeit there are questions about its extent and exclusive orgin from the primary area in different species (Feliciano, 1995; Feliciano et al., 1995; Weedman and Ryugo, 1996a,b; Schofield and Coomes, 2005). The cortical fibers form asymmetric synaptic junctions with granule cells but the contacts occur at the periphery - rather than the center - of *bona fide* glomeruli (Meltzer and Ryugo, 2006), while the projection from the auditory regions of the pontine nuclei was in the form of mossy terminals. Cognitive processing could thus directly modulate granule cell firing, perhaps making them more responsive to mossy fiber inputs. This kind of synaptic interaction, which as far as we know is absent in cerebellum, sharply distinguishes the microcircuit of the GCS in the CN from that in the cerebellar granular layer. Nevertheless, the paucity of data makes it still an open question whether the direct cortical projection also impinges upon UBCs and gives raise to at least a small numbe of CN mossy fibers.

Thus, in spite of the continuity of the territories that make up the GCS, clear examples have been provided for different patterns of innervation of granule cell areas, ranging from widespread projections to differential terminations and clustering of afferents. In analogy with the cerebellar cortex (Diño et al., 1999), pontine mossy fibers synapse with granule cells in the glomeruli of the GCS, with the exception of the DCN, but seem to avoid UBCs, perhaps as the result of repulsive factors as suggested.

In sum, our immunocytochemical study, in conjunction with published hodological data, demonstrates co-distribution of granule cells and UBCs in most regions of the CN and strongly suggests that both of these two types of excitatory interneurons are targeted by most of the projections to the GCS, with the likely exception of the pontine afferents, the type II primary cochlear fibers and perhaps also other inputs yet to be analyzed in sufficient detail.

Comparative anatomical considerations

As pointed out by Farago et al., (2006) the separate embryonic origins of the granule cell systems of the CN and the cerebellum along the rostrocaudal axis of the rhombencephalon favors their separate derivation through “evolutionary convergence upon a primary organization that is likely advantageous for accomplishing similar computations, albeit to different specific ends”. Indeed, the GCS of the CN is extraordinarily developed in certain mammals without concomitant, corresponding enlargement of the vestibulocerebellum (Merzenich et al., 1973). Data from the literature indicate that the GCS is a conserved feature of the mammalian CN, albeit with prominent variations in volume relative to other CN divisions and deployment of the granule neurons. Possible concomitant variations in the maps of the UBCs – as well as their putative forms termed shrub, mitt and chestnut cells – may be obtainable using the cell population markers adopted in this study. It is already known that UBCs occur in the CN of several mammalian species in addition to rat and mouse - Mugnaini and Floris, 1994; Idrizbegovic et al., 2001; chincilla – Hutson and Morest, 1996; guinea pig – Winsky and Jacobowitz, 1995, Caicedo et al., 1996; Alibardi, 2003b; ferret –Fuentes-Santamaria et al., 2005; cat – Brawer et al., 1974; common marmoset and vervet monkeys -Spatz, 1999, 2000; human - Spatz, 2001). Given the substantial phylogenetic diversity in the organization of the

auditory brainstem, comparative maps of the distribution of granule cells, UBCs and their mossy fiber afferents are likely to reveal interspecies differences that may clarify the division of the cell population in subsets expressing different chemical and morphological phenotypes.

In particular, the lamination of the DCN and the structure of the GCS present conspicuous diversity in primates, with a tendency for the granule cells to condense beneath the ependyma at the surface of the molecular layer (Moore and Osen, 1979; Moore, 1980; Heiman-Patterson and Strominger, 1985). While the adult human CN contains scattered granule cells and UBCs (Heiman-Patterson and Strominger, 1985; Spatz, 2001), the granular layer is prominent in the fetus and rapidly decreases in the infant; this process of cell elimination could possibly be involved in engendering changes of the major cell types in the DCN that have been reported previously (Moore, 1980; Heiman-Patterson and Strominger, 1985; Terr and Edgerton, 1985; Adams, 1986), but are still to be clarified. Renewed comparative investigations may therefore help elucidate the precise mechanisms by which optimal auditory performance is attained across species.

Concluding remarks

In conclusion, the CN contains UBCs, most, if not all, of which are $Eps8^+$ and $Trb2^+$. They are distributed in all regions of the GCS and are especially numerous in the DCN and the subpeduncular corner. The CN UBCs form two main chemically distinct subsets, one expressing mGluR1α and the other CR, which share the same morphological features. In view of the profound similarities between cerebellar and CN UBCs, we presume that all UBC axons form an intrinsic system of mossy fibers synapsing with granule cells and other UBCs, although the existence of other targets cannot be ruled out. Notably, Doucet and Ryugo (1997) and Alibardi (2004) retrogradely labeled UBCs in DCN and VCN after tracer injections in the DCN, and it is likely that CN's UBCs act both locally and at a distance. UBCs are likely to share with granule cells most of the inputs to the GCS. Because of their strong, AMPA- and NMDA-mediated synaptic linkage to individual mossy fibers (Rossi et al., 1995; Nunzi et al., 2001), the UBCs would engender temporal expansion of "private line"connections for separate afferent channels leading into the DCN. As the brush is usually innervated by an individual mossy fiber terminal, by synchronizing the firing of numerous granule cells and amplifying the functional impact of an individual input, an enrichment of UBCs would effectively regulate the activity of stellate, cartwheel, pyramidal and tuberculoventral cells, integrating frequency related auditory input carried by descending branches of primary cochlear fibers with somatosensory information from head and neck and auditory information processed by other neurons in VCN, upper brainstem auditory centers, and the cerebral cortex.

We propose therefore, that the UBC is a neuron type of primary importance in the microcircuits of the CN of all the mammals that possess a well-developed GCS, as it is in the vestibulocerebellum. Further elucidation of its intrinsic properties and synaptic connections could be helpful towards a full understanding of the functional ranges of the eight cranial nerve, the CN, and its many afferents, and perhaps also contribute to improvements of brain stem auditory prostheses.

Supplementary Material

Refer to Web version on PubMed Central for supplementary material.

Acknowledgments

This study was supported by PHS RO1 grant NS 09904 to E M. The authors wish to thank Dr. R. Shigemoto for the generous gift of mGluR1a antiserum.

List of abbreviations used in the main text

Anr	auditory nerve root
AVCN	anteroventral cochlear nucleus
BSA	bovine serum albumin
CN	coclear nuclear complex
CR	calretinin
DAB	3,3-diaminobenzidine hydrochloride
DCN	dorsal cochlear nucleus
Eps8	epidermal growth factor substrate 8
$GABA_A$	gamma-aminobutyric acid receptor A
GCS	granule cell system
mGluR1α	metabotropic glutamate receptor 1α
NGS	normal goat serum
PB	phosphate buffer
PBS	phosphate buffered saline
PVCN	posteroventral cochlear nucleus
SCC	small cell cap
Tbr2	T-box gene Tbr2
Tris	hydroxymethyl aminomethane
TBS	Tris-bufferes saline
TBS-T	Tris-buffered saline with added Triton-X100
VCN	ventral cochlear nucleus
UBC	unipolar brush cell
vnr	vestibular nerve root

References

Adams JC. Neuronal morphology in the human cochlear nucleus. Arch Otolaryngol Head Neck Surg 1986;112:1253–1261. [PubMed: 3533119]

Alibardi L. Immunocytochemistry of glycine in small neurons of the granule cell areas of the guinea pig dorsal cochlear nucleus: a post-embedding ultrastructural study. Histochem J 2002;34:423–434. [PubMed: 12814190]

Alibardi L. Ultrastructural immunocytochemistry for glycine in neurons of the dorsal cochlear nucleus of the guinea pig. J Submicrosc Cytol Pathol 2003a;35:373–387. [PubMed: 15137679]

Alibardi L. Ultrastructural distribution of glycinergic and GABAergic neurons and axon terminals in the rat dorsal cochlear nucleus, with emphasis on granule cell areas. J Anat 2003b;203:31–56. [PubMed: 12892405]

Alibardi L. Mossy fibers in granule cell areas of the rat dorsal cochlear nucleus from intrinsic and extrinsic origin innervate unipolar brush cell glomeruli. J Submicrosc Cytol Pathol 2004;36:193–210. [PubMed: 15554505]

Alibardi L. Review: cytological characteristics of commissural and tuberculo-ventral neurons in the rat dorsal cochlear nucleus. Hear Res 2006;216–217:73–80.

Altman J, Bayer SA. Time of origin and distribution of a new cell type in the rat cerebellar cortex. Exp Brain res 1977;29:265–274. [PubMed: 913518]

Altman, J.; Bayer, SA. Development of the cerebellar system. Boca Raton, FL: CRC press; 1996.

Anderson LA, Malmierca MS, Wallace MN, Palmer AR. Evidence for a direct, short latency projection from the dorsal cochlear nucleus to the auditory thalamus in the guinea pig. Eur J Neurosci 2006;24:491–498. [PubMed: 16836634]

Arai R, Winsky L, Arai M, Jacobowitz DM. Immunohistochemical localization of calretinin in the rat hindbrain. J Comp Neurol 1991;310:21–44. [PubMed: 1939729]

Aruga J, Yokota N, Hashimoto M, Furuichi T, Fukuda M, Mikoshiba K. A novel zinc finger protein, zic, is involved in neurogenesis, especially in the cell lineage of cerebellar granule cells. J Neurochem 1994;63:1880–1890. [PubMed: 7931345]

Balakrishnan V, Trussell LO. Synaptic inputs to granule cells of the dorsal cochlear nucleus. J Neurophysiol. 2007 (e-publication ahead of print).

Bahn S, Jones A, Wisden W. The intrinsic specification of gamma-aminobutyric acid type A receptor alpha6 subunit gene expression in cerebellar granule cells. Eur J Neurosci 1997;11:2194–2198. [PubMed: 10336690]

Barmack NH, Baughman RW, Errico P, Shojaku H. Vestibular primary afferent projections to the cerebellum of the rabbit. J Comp Neurol 1993;327:521–534. [PubMed: 7680050]

Batini C, Compoint C, Buisseret-Delmas C, Daniel H, Guegan M. Cerebellar nuclei and the nucleocortical projections in the rat: retrograde tracing coupled to GABA and glutamate immunohistochemistry. J Comp Neurol 1992;315:74–84. [PubMed: 1371781]

Behrens EG, Schofield BR, Thompson AM. Aminergic projections to the cochlear nucleus via descending auditory pathways. Brain Res 2002;955:34–44. [PubMed: 12419519]

Bell CC. Memory-based expectations in electrosensory systems. Curr Op Neurobiol 2001;11:481–587. [PubMed: 11502396]

Bell CC. Evolution of cerebellum-like structures. Brain Behav Evol 2002;59:312–326. [PubMed: 12207086]

Benson TE, Brown MC. Postsynaptic targets of type II auditory nerve fibers in the cochlear nucleus. J Assoc Res Otolaryngol 2004;25:111–125. [PubMed: 15357415]

Berglund AM, Benson TE, Brown MC. Synapses from labeled type II axons in thew mouse cochlear nucleus. Hearing Res 1996;75:121–130.

Berrebi AS, Mugnaini E. Effects of the murine mutation ‘nervous’ on neurones in cerebellum and dorsal cochlear nucleus. J Neurocytol 1988;17:465–484. [PubMed: 3193127]

Berrebi AS, Morgan JI, Mugnaini E. The Purkinje cell class may extend beyond the cerebellum. J Neurocytol 1990;19:643–654. [PubMed: 2077109]

Berrebi AS, Mugnaini E. Distribution and targets of the cartwheel cell axon in the dorsal cochlear nucleus of the guinea pig. Anat Embryol 1991;183:427–454. [PubMed: 1862946]

Berrebi, AS.; Mugnaini, E. Alterations in the dorsal cochlear nucleus of cerebellar mutant mice. In: Merchán, MA.; Juiz, JM.; Godfrey, DA.; Mugnaini, E., editors. The Mammalian Cochlear Nuclei: Organization and Function. Vol. 239. New York: NATO ASI Series; 1993. p. 107-119.

Bilak SR, Morest DK. Differential expression of the metabotropic glutamate receptor mGluR1α by neurons and axons in the cochlear nucleus: in situ hybridization and immunocytochemistry. Synapse 1998;28:251–270. [PubMed: 9517834]

Blackstad TW, Osen KK, Mugnaini E. Pyramidal neurones of the dorsal cochlear nucleus: A Golgi and computer reconstruction study in cat. Neuroscience 1984;13:827–854. [PubMed: 6527780]

Boehm SL II, Homanics GE, Blednov YA, Harris RA. δ-subunit containing $GABA_A$ receptor knockout mice are less sensitive to the actions of 4,5,6,7-tetrahydroisoxazolo-[5,4-c]pyridin-3-ol. Eur J Pharmacol 2006;541:158–162. [PubMed: 16777089]

Brawer JR, Morest DK, Kane EC. The neuronal architecture of the cochlear nucleus of the cat. J Comp Neurol 1974;160:491–506. [PubMed: 1091667]

Burian M, Gstoettner W. Projection of primary vestibular afferent fibres to the cochlear nucleus in the guinea pig. Neurosci Lett 1988;84:13–7. [PubMed: 2831482]

Bukowska D. Morphological evidence for secondary vestibular afferent connections to the dorsal cochlear nucleus in the rabbit. Cells Tissues Organs 2002;170:61–68. [PubMed: 11602803]

Caicedo A, Herbert H. Topographiy of descending projections from the inferior colliculus to auditory brainstem nuclei in the rat. J Comp Neurol 1993;328:377–392. [PubMed: 7680052]

Caicedo A, d'Aldin C, Puel JL, Eybalin M. Distribution of calcium-binding protein immunoreactivities in the guinea pig auditory brainstem. Anat Embryol 1996;194:465–487. [PubMed: 8905014]

Campbell HR, Meek J, Zhang J, Bell CC. Anatomy of the posterior caudal lobe of the cerebellum and the eminentia granularis posterior in a mormyrid fish. J Comp Neurol 2007;502:714–735. [PubMed: 17436286]

Campos ML, De Cabo C, Wisden W, Juiz JM, Merlo D. Expression of $GABA_A$ receptor subunits in rat braistem auditory pathways: cochlear nuclei, superior olivary complex and nuclei of the lateral lemniscus. Neuroscience 2001;102:625–638. [PubMed: 11226699]

Cant, NB. The cochlear nucleus: neuronal types and their synaptic organization. In: Webster, DB.; Popper, AN.; Fay, RR., editors. The Mammalian Auditory Pathway: Neuroanatomy, vol 1 Springer Handbook of Auditory Research. New York: Springer-Verlag; 1992. p. 66p. 6-116.

Cant NB, Benson CG. Parallel auditory pathways: projection patterns of the different neuronal populations in the dorsal and ventral cochlear nuclei. Brain Res Bull 2003;60:457–474. [PubMed: 12787867]

Cant NB, Morest DK. Axons from non-cochlear sources in the anteroventral cochlear nucleus of the cat. A study with the rapid Golgi method. Neuroscience 1978;3:1003–1029. [PubMed: 85282]

Crook J, Hendrikson A, Robinson FR. Colocalization of glycine and gaba immunoreactivities in interneurons in macaca monkey cerebellar cortex. Neuroscience 2006;141:1951–1959. [PubMed: 16784818]

DeCamilli P, Miller PF, Levitt P, Walter U, Greengard P. Anatomy of cerebellar Purkinje cells in the rat determined by a specific immunohistochemical marker. Neuroscience 1984;11:761–817. [PubMed: 6330609]

de Diego I, Kyriakopoulou K, Karagogeos D, Wassef M. Multiple influences on the migration of precerebellar neurons in the caudal medulla. Development 2002;129:297–306. [PubMed: 11807023]

Devor A. Is the cerebellum like cerebellar-like structures? Brain Res Rev 2000;34:149–156. [PubMed: 11113505]

Devor A. The great gate: control of sensory information flow to the cerebellum. Cerebellum 2002;1:27–34. [PubMed: 12879971]

Diana MA, Otsu Y, Maton G, Collin T, Chat M, Dieudonné S. T-type and L-type Ca^{2+} conductances define and encode the bimodal furing patter of vestibulocerbellar unipolar brush cells. J Neurosci 2007;27:3823–3838. [PubMed: 17409247]

Diño MR, Nunzi MG, Anelli R, Mugnaini E. Unipolar brush cells in the vestibulocerebellum: afferents and targets. Prog Brain Res 2000a;124:123–137.

Diño MR, Schruerger RJ, Liu JB, Slater NT, Mugnaini E. Unipolar brush cell: a potential feedforward excitatory interneuron of the cerebellum. Neuroscience 2000b;98:625–636.

Diño MR, Perachio AA, Mugnaini E. Cerebellar unipolar brush cells are targets of primary vestibular afferents: an experimental study in gerbil. Exp Brain Res 2001;140:162–170. [PubMed: 11521148]

Diño MR, Willard FH, Mugnaini E. Distribution of unipolar brush cells and other calretinin immunoreactive components in the mammalian cerebellar cortex. J Neurocytol 1999;28:99–126. [PubMed: 10590511]

Doucet JR, Ryugo DK. Projections from the ventralcochlear nucleus to the dorsal cochlear nucleus in rats. J Comp Neurol 1997;385:245–264. [PubMed: 9268126]

Dugué GP, Dumoulin A, Triller A, Dieudonné S. Target-dependent use of co-released inhibitory transmitters at central synapses. J Neurosc 2005;25:6490–6498.

Dunn, ME.; Vetter, DE.; Berrebi, AS.; Krider, HM.; Mugnaini, E. Advances in Speech, Hearing and Language Processing. Vol. 3. London: JAI Press; 1996. The mossy fiber–granule cell–cartwheel cell system in the mammalian cochlear nuclear complex; p. 63-87.

Englund C, Kowalczyk T, Daza RA, Dagan A, Lau C, Rose MF, Hevner RF. Unipolar brush cells of the cerebellum are produced in the rhombic lip and migrate through developing white matter. J Neurosci 2006;26:9184–9195. [PubMed: 16957075]

Farago AF, Awatramani RB, Dymecki SM. Assembly of the brainstem cochlear nuclear complex is revealed by intersectional and subtractive genetic fate maps. Neuron 2006;50:205–218. [PubMed: 16630833]

Fekete DM, Rouiller EN, Liberman MC, Ryugo DK. The central projectins of intracellularly labeled auditory nerve fibers in cats. J Comp Neurol 1984;229:432–450. [PubMed: 6209306]

Feliciano, M. Descending projections from the auditory neocortex to midbrain and brainstem auditory nuclei: A neuroscheical and light microscopic study. Storrs: The University of Connecticut; 1995. Thesis

Feliciano M, Saldaña E, Mugnaini E. Direct projections from the rat primary auditory neocortex to nucleus sagulum, paralemniscal regions, superior olivary complex and cochlear nuclei. Aud Neurosci 1995;1:287–308.

Ferragamo MJ, Golding NL, Gardner SM, Oertel D. Golgi cells in the superficial granule cell domain overlying the ventral cochlear nucleus: morphology and electrophysiology in slices. J Comp Neurol 1998;400:519–528. [PubMed: 9786412]

Floris A, Diño M, Jacobowitz DM, Mugnaini E. The unipolar brush cells of the rat cerebellar cortex and cochlear nucleus are calretinin-positive: a study by light and electron microscopic immunocytochemistry. Anat Embryol 1994;189:495–520. [PubMed: 7978355]

Friedland DR, Popper P, Eernisse R, Cioffi JA. Differentially expressed genes in the rat cochlear nucleus. Neuroscience 2006;142:753–768. [PubMed: 16905270]

Fuentes-Santamaria V, Alvarado JC, Taylor AR, Brunso-Bechtold JK, Henkel CK. Quantitative changes in calretinin immunostaining in the cochlear nuclei after unilateral cochlear removal in younf ferrets. J Comp Neurol 2005;483:458–475. [PubMed: 15700274]

Fünfschilling U, Reichardt LF. Cre-mediated recombination in rhombic lip derivatives. Genesis 2002;33:160–169. [PubMed: 12203913]

Gómez-Nieto R, Rubio ME, López DE. Cholinergic input from the ventral nucleus of the trapezoid body to cochlear root neurons in rats. J Comp Neurol 2007;506:452–468.

Haenggeli CA, Pongstaporn T, Doucet JR, Ryugo DK. Projections from the spinal trigeminal nucleus to the cochlear nucleus in the rat. J Comp Neurol 2005;484:191–205. [PubMed: 15736230]

Hackney CM, Osen KK, Kolston J. Anatomy of the cochlear nuclear complex of guinea pig. Anat Embryol 1990;182:123–149. [PubMed: 2244686]

Heiman-Patterson TD, Strominger NL. Morphological changes in the cochlear nuclear complex in primate phylogeny and development. J Morphol 1985;186:289–306. [PubMed: 4087302]

Hoshino M. Molecular machinery governing GABAergic neuron specification in the cerebellum. Cerebellum 2006;5:193–198. [PubMed: 16997750]

Howell DN, Morgan WJ, Jarjour AA, Spirou GA, Berrebi AS, Kennedy TE, Mathers PH. Molecular guidance cues necessary for axon pathfinding from the ventral cochlear nucleus. J Comp Neurol 2007;504:533–549. [PubMed: 17701984]

Hurd LB, Hutson KA, Morest DK. Cochlear nerve projections to the small cell shell of the cochlear nucleus: the neuroanatomy of extremely thin sensory axons. Synapse 1999;33:83–117. [PubMed: 10400889]

Hutson KA, Morest DK. Fine structure of the cell clusters in the cochlear nerve root: stellate, granule, and mitt cells offer insights into the synaptic organization of local circuit neurons. J Comp Neurol 1996;371:397–414. [PubMed: 8842895]

Ibrahim M, Menoud PA, Celio MR. Neurones in the adult rat anterior medullary velum. J Comp Neurol 2000;419:122–134. [PubMed: 10717643]

Idrizbegovic E, Canlon B, Bross LS, Willot JF, Bogdanovic N. The total number of neurons and calcium binding protein positive neurons during aging in the cochlear nucleus of CBA/Ca mice: a quantitative study. Hear Res 2001;158:102–115. [PubMed: 11506942]

Ilijic E, Guidotti A, Mugnaini E. Moving up or moving down? Malpositioned cerebellar unipolar brush brush cells in reeler mouse. Neuroscience 2005;136:633–467. [PubMed: 16344141]

Irie T, Kukui I, Ohmori H. Activation of GIRK channels by muscarinic receptors and group II metabotropic glutamate receptors suppresses Golgi cell activity in the cochlear nucleus of mice. J Neurophysiol 2006;96:2633–2644. [PubMed: 16855110]

Ito M. Cerebellar circuitry as a neuronal machine. Prog Neurobiol 2006;78:272–303. [PubMed: 16759785]

Itoh K, Kamiya H, Mitani A, Yasui Y, Takada M, Mizuno N. Direct projections from the dorsal column nuclei and the spinal trigeminal nuclei to the cochlear nuclei in the cat. Brain Res 1987;400:145–150. [PubMed: 2434184]

Ivanova A, Yuasa S. Neuronal migration and differentiation in the development of the mouse dorsal cochlear nucleus. 1998;20:495–511.

Jaarsma D, Diño M, Ohishi H, Shigemoto R, Mugnaini E. Metabotropic glutamate receptors are associated with non-synaptic appendages of unipolar brush cells in rat cerebellar cortex and cochlear nuclear complex. J Neurocytol 1998;27:303–327. [PubMed: 9923978]

Josephson EM, Morest DK. Synaptic nests lack glutamate transporters in the cochlear nucleus of the mouse. Synapse 2003;49:29–46. [PubMed: 12710013]

Joyner AL, Zervas M. Genetic inducible fate mapping in mouse: establishing genetic lineages and defining genetic neuroanatomy in the nervous system. Dev Dyn 2006;235:2376–2385. [PubMed: 16871622]

Kalinichenko SG, Okhotin VE. Unipolar brush cells--a new type of excitatory interneuron in the cerebellar cortex and cochlear nuclei of the brainstem. Neurosci Behav Physiol 2005;35:21–36. [PubMed: 15739785]

Kane ES. Descending inputs to the cat dorsal cochlear nucleus: an electron microscopic study. J Neurocytol 1977;6:583–605. [PubMed: 925723]

Kato K. Novel $GABA_A$ receptor alpha subunit is expressed only in cerebellar granule cells. J Mol Biol 1990;214:619–624. [PubMed: 2167378]

Kevetter GA, Perachio AA. Projections from the sacculus to the cochlear nuclei in the Mongolian gerbil. Brain Behav Evol 1989;34:193–200. [PubMed: 2590835]

Korada S, Schwartz IR. Calcium binding proteins and the AMPA glutamate receptor subunits in gerbil cochlear nucleus. Hear Res 2000;140:23–37. [PubMed: 10675633]

Korte GE, Mugnaini E. The cerebellar projection of the vestibular nerve in the cat. J Comp Neurol 1979;184:265–278. [PubMed: 762284]

Laurie DJ, Seeburg PH, Wisden W. The distribution of 13 $GABA_A$ receptor subunit mRNAs in the rat brain. II. Olfactory bulb and cerebellum. J Neurosci 1992;12:1063–1076. [PubMed: 1312132]

Li H, Mizuno N. Single neurons in the spinal trigeminal and dorsal column nuclei project to both the cochlear nucleus and the inferior colliculus by way of axon collaterals: a fluorescent retrograde double-labeling study in the rat. Neurosci Res 1997;29:135–142. [PubMed: 9359462]

Lohmann C, Friauf E. Distribution of the calcium-binding proteins parvalbumin and calretinin in the auditory brainstem of adult and developing rats. J Comp Neurol 1996;367:90–109. [PubMed: 8867285]

Lorente de Nó, R. The Primary Acoustic Nuclei. New York: Raven Press; 1981.

Machold R, Fishell G. *Math1* is expressed in temporally discrete pools of cerebellar rhombic lip neural progenitors. Neuron 2005;48:17–24. [PubMed: 16202705]

Malmierca MS. The structure and physiology of the rat auditory system: an overview. Int Rev Neurobiol 2003;56:147–211. [PubMed: 14696313]

Malmierca MS, LeBeau FEN, Rees A. The topographical organization of descending projections from the central nucleus of the inferior colliculus in the guinea pig. Hearing Res 1996;93:167–180.

McCue MP, Guinan JJ Jr. Influence of efferent stimulation on acoustically responsive vestibular afferents in the cat. J Neurosci 1994;14:6071–6083. [PubMed: 7931563]

McDonald DM, Rasmussen GL. Ultrastructural characteristics of synaptic endings in the cochlear nucleus having acetylcholinesterase activity. Brain res 1971;28:1–18. [PubMed: 4104277]

Meltzer NE, Ryugo DK. Projections from auditory cortex to cochlear nucleus: A comparative analysis of rat and mouse. Anat Rec 2006;288:397–408.

Merchán MA, Collia FP, Merchán JA, Saldaña E. Distribution of primary afferent fibres in the cochlear nuclei. A silver and horseradish peroxidase (HRP) study. J Anat 1985;141:121–30. [PubMed: 4077711]

Merchán MA, Collia FP, Merchán JA, Ludena MD. Distribution of primary cochlear afferents in the bulbar nuclei of the rat: a horseradish peroxidase (HRP) study in parasagittal sections. J Anat 1986;144:71–80. [PubMed: 3319993]

Merzenich MM, Kitzes L, Aitkin L. Anatomical and physiological evidence for auditory specialization in the mountain beaver (*Aplondontia reifa*). Brain Res 1973;58:331–344. [PubMed: 4756133]

Moore JK. The primate cochlear nuclei; loss of lamination as phylogenetic process. J Comp Neurol 1980;193:609–629. [PubMed: 6777412]

Moore JK. The human auditory brain stem: a comparative view. Hearin Res 1987;29:1–32.

Moore, JK. Cholinergic, GABA-ergic, and noradrenergic input to cochlear granule cells in the guinea pig and monkey. In: Sika, J.; Masterton, RB., editors. Auditory pathway: structure and function. New York: Plenum; 1988. p. 123-131.

Moore JK, Osen KK. The cochlear nuclei in man. Am J Anat 1979;154:393–418. [PubMed: 433789]

Moore JK, Osen KK, Storm-Mathisen J, Ottersen OP. Gamma-aminobutyric acid and glycine in the baboon cochlear nuclei: an immunocytochemical colocalization study with reference to interspecies differences in inhibitory systems. J Comp Neurol 1996;369:497–519. [PubMed: 8761924]

Montgomery JC, Coombs S, Conley RA, Bodznick D. Hindbrain sensory processing in lateral line, electrosensory and auditory systems: a comparative overview of anatomical and functional similarities. Aud Neurosci 1995;1:207–231.

Morales D, Hatten ME. Molecular markers of neuronal progenitors in the embryonic cerebellar anlage. J Neurosci 2006;26:12226–12236. [PubMed: 17122047]

Morest, DK. Structural basis for signal processing: challenge of the synaptic nests. In: Syka, J., editor. Acoustical signal processing in the central auditory system. New York: Plenum Press; 1997. p. 19-32.

Morin F, Diño MR, Mugnaini E. Postnatal Differentiation of the dendritic brush of the unipolar brush cell and its synapses in rat cerebellum. Neuroscience 2001;104:1127–1139. [PubMed: 11457596]

Moskowitz N. Comparative aspects of some features of central auditory system of primates. Ann New York Acad Sci 1969;167:357–367.

Mugnaini E. GABA neurons in the superficial layers of the rat dorsal cochlear nucleus: Light and electron microscopic immunocytochemistry. J Comp Neurol 1985;235:61–81. [PubMed: 3886718]

Mugnaini, E. GABAergic inhibition in the Cerebellar System. In: Martin, DL.; Olsen, RW., editors. GABA in the Nervous System: The View at Fifty Years. Philadelphia: Lippicott Williams &Wilkins; 2000. p. 383-407.

Mugnaini E, Diño R, Jaarsma D. The unipolar brush cells of the mammalian cerebellum and cochlear nucleus: cytology and microcircuitry. Progr Brain Res 1997;114:131–150.

Mugnaini E, Floris A. The unipolar brush cell: The neglected neuron of the mammalian cerebellar cortex. J Comp Neurol 1994;339:174–180. [PubMed: 8300904]

Mugnaini E, Floris A, Wright-Goss M. Extraordinary synapses of the unipolar brush cell: An electron microscopic study in the rat cerebellum. Synapse 1994;16:284–311. [PubMed: 8059339]

Mugnaini E, Forströnen PF. Ultrastructural studies on the cerebellar histogenesis. I. Differentiation of granule cells and development of glomeruli in the chick embryo. Zeit Zellforsch 1967;77:115–143.

Mugnaini E, Maler L. Comparison between the fish electrosensory lateral line lobe and the mammalian dorsal cochlear nucleus. J Comp Physiol A 1993;173:683–685.

Mugnaini E, Morgan JI. The neuropeptide cerebellin is a marker for two similar neuronal circuits in rat brain. Proc Nat Acad Sci USA 1987;84:8692–8696. [PubMed: 3317418]

Mugnaini E, Osen KK, Dahl A-L, Friedrich VL Jr, Korte G. Fine structure of granule cells and related interneurons (termed Golgi cells) in the cochlear nuclear complex of cat, rat and mouse. J Neurocytol 1980a;9:537–570. [PubMed: 7441303]

Mugnaini E, Warr WB, Osen KK. Distribution and light microscopic features of granule cells in the cochlear nuclei of cat, rat and mouse. J Comp Neurol 1980b;191:581–606. [PubMed: 6158528]

Newlands SD, Perachio AA. central projections of the vestibular nerve: a review and single fiber study in the Mongolian gerbil. Brain Res Bull 2003;60:475–495. [PubMed: 12787868]

Nunzi MG, Mugnaini E. Unipolar brush cell axons form a large system of intrinsic mossy fibers in the postnatal vestibulocerebellum. J Comp Neurol 2000;422:55–65. [PubMed: 10842218]

Nunzi MG, Birnstiel S, Bhattacharyya B, Slater NT, Mugnaini E. Unipolar brush cells form a glutamatergic projection system within the mouse cerebellar cortex. J Comp Neurol 2001;434:329–341. [PubMed: 11331532]

Nunzi MG, Shigemoto R, Mugnaini E. Differential expression of calretinin and metabotropic glutamate receptor mGluR1α defines subpopulations of unipolar brush cell populations in mouse cerebellum. J CompNeurol 2002;451:189–199.

Nunzi MG, Russo M, Mugnaini E. Vesicular glutamate transporters VGLUT1 and VGLUT2 define two subsets of unipolar brush cells in mouse vestibulocerebellum. Neuroscience 2003;122:359–371. [PubMed: 14614902]

Nunzi MG, Fung C, Mugnaini E. Differential distributions of two subsets of unipolar brush cells in the cerebellar cortex of the Rhesus monkey. Soc Neurosci Abstr Atlanta (GA). 2006

Nusser Z, Sieghart W, Stephenson FA, Somogyi P. The alpha 6 subunit of the $GABA_A$ receptor is concentrated in both inhibitory and excitatory synapses on cerebellar granule cells. J Neurosci 1996;16:103–114. [PubMed: 8613776]

Oertel D, Young ED. What's a cerebellar circuit doing in the auditory system? Trends Neurosci 2004;27:104–110. [PubMed: 15102490]

Offenhauser N, Castelletti D, Mapelli L, Soppo BE, Regondi MC, Rossi P, D'Angelo E, Frassoni C, Amadeo A, Tocchetti A, Pozzi B, Disanza A, Guarnieri D, Betsholtz C, Scita G, Heberlein U, Di Fiore PP. Increased ethanol resistance and consumption in Eps8 knockout mice correlates with altered actin dynamics. Cell 2006;127:213–26. [PubMed: 17018287]

Ohlrogge M, Doucet JR, Ryugo DK. Projections of the pontine nuclei to the cochlear nucleus in rats. J Comp Neurol 2001;436:290–303. [PubMed: 11438931]

Osen KK. Cytoarchitecture of the cochlear nuclei in the cat. J Comp Neurol 1969;136:453–484. [PubMed: 5801446]

Osen KK, Jansen J. The cochlear nuclei in the common porpoise, *Phocaena phocaena*. J Comp Neurol 1965;125:223–257. [PubMed: 5852851]

Osen KK. Course and termination of the primary afferents in the cochlear nuclei of the cat. Arch Ital Biol 1970;108:21–51. [PubMed: 5438720]

Osen, KK.; Mugnaini, E. Neuronal circuits in the dorsal cochlear nucleus. In: Syka, J.; Aitkin, L., editors. Neuronal Mechanisms of Hearing. New York: Plenum Press; 1981. p. 119-125.

Osen KK, Mugnaini E, Dahl AL, Chistiansen AH. Histochemical localization of acetylcholinesterase in the cochlear and superior olivary nuclei: A reappraisal with emphasis on the cochlear granule cell system. Arch Ital Biol 1984;122:169–212. [PubMed: 6517650]

Palay, SL.; Chan-Palay, V. Cytology and organization. New York: Springer; 1974. Cerebellar cortex.

Pasqualetti M, Diáz C, Renaud JS, Rijli FM, Glover JC. Fate-mapping the mammalian hindbrain: segmental origins of vestibular projection neurons assessed using rhombomere-specific *hoxa2* enhancer elements in mouse embryo. J Neurosci 2007;27:9670–9681. [PubMed: 17804628]

Paxinos, G.; Watson, C. The Rat Brain in Stereotaxic Coordinates. 4. S. Diego: Academic Press; 1998.

Paxinos, G.; Carrive, P.; Wang, H.; Wang, PY. Chemoarchitectonic Atlas of the Rat Brain Stem S. Diego: Academic Press; 1999.

Peng Z, Huang CS, Stell BM, Mody I, Houser CR. Altered expression of the δ subunit of the $GABA_A$ receptor in a mouse model of temporal lobe epilepsy. J Neurosci 2004;24:8629–8639. [PubMed: 15456836]

Peters, A.; Palay, SL.; Webster de, FH. The fine structure of the nervous system. New York: Oxford University Press; 1991.

Petralia RS, Wang YX, Zhao HM, Wenthold RL. Ionotropic and metabotropic glutamate receptors show unique postsynaptic, presynaptic, and glial localizations in the dorsal cochlear nucleus. J Comp Neurol 1966;372:356–383. [PubMed: 8873866]

Pfaller K, Arvidsson J. central distribution of trigeminal and upper cervical afferents in the rat studied by anterograde transport of horseradish peroxidase conjugated to wheat germ agglutinin. J Comp Neurol 1988;268:91–108. [PubMed: 3346387]

Pór A, Pocsai K, Rusznak Z, Szucs G. Presence and distribution of three calcium binding proteins in projection neurons of the adult rat cochlear nucleus. Brain Res 2005;1039:63–74. [PubMed: 15781047]

Quinn B, Graybiel AM. A differentiated silver intensification procedure for the peroxidase-diaminobenzidine reaction. J Histochem Cytochem 1996;44:71–74. [PubMed: 8543785]

Rogers JH, Résibois A. Calretinin and calbindin-D28k in rat brain: patterns of partial co-localization. Neuroscience 1992;51:843–865. [PubMed: 1488126]

Rodrigo J, Fernandez AP, Serrano J, Monzon M, Monleon E, Badiola JJ, Climent S, Martinez-Murillo R, Martinez A. Distribution and expression pattern of the nitrergic system in the cerebellum of the sheep. Neuroscience 2006;139:889–898. [PubMed: 16533568]

Rossi DJ, Alford S, Mugnaini E, Slater NT. Properties of transmission at a giant glutamatergic synapse in cerebellum: the mossy fiber-unipolar brush cell synapse. J Neurophysiol 1995;74:24–42. [PubMed: 7472327]

Rossi DJ, Hamann M. Spillover-mediated transmission at inhibitory synapses promoted by high affinity α6 subunit $GABA_A$ receptors and glomerular geometry. Neuron 1998;20:783–795. [PubMed: 9581769]

Rouiller EM, Cronin-Schreiber R, Fekete DM, Ryugo DK. The central projections of intracellularly labeled auditory nerve fibers in cats: an analysis of terminal morphology. J Comp Neurol 1986;249:261–278. [PubMed: 3734159]

Russo MJ, Mugnaini E, Martina M. Intrinsic properties and mechanisms of spontaneous firing in mouse cerebellar unipolar brush cells. J Physiol 2007;581:709–724. [PubMed: 17379636]

Rusznak Z, Forsythe ID, Brew HM, Stanfield PR. Membrane currents influencing action potential latency in granule neurons of the rat cochlear nucleus. Eur J Neurosci 1997;9:2348–2358. [PubMed: 9464929]

Ryugo DK, Haenggeli CA, Doucet JR. Multimodal inputs to the granule cell domain of the cochlear nucleus. Exp Brain Res 2003;153:477–485. [PubMed: 13680048]

Ryugo DK, Parks TN. Primary innervation of the avian and mammalian cochlear nucleus. Brain Res Bull 2003;60:435–456. [PubMed: 12787866]

Saldaña, E. Descending projections from the inferior colliculus to the cochlear nuclei in mammals. In: Merchan, MA.; Juiz, JM.; Godfrey, DA.; Mugnaini, E., editors. The mammalian cochlear nuclei: organization and function. New York: Plenum; 1993. p. 153-165.

Saldaña E, Feliciano M, Mugnaini E. Distribution of descending projections from primary auditory neocortex to inferior colliculus mimics the topography of intracollicular projections. J Comp Neurol 1996;371:15–40. [PubMed: 8835717]

Salero E, Hatten ME. Differentiation of ES cells into cerebellar neurons. Proc Nat Acad Sci USA 2007;104:2997–3002. [PubMed: 17293457]

Saul SM, Brzezinski JA IV, Altschuler RA, Shore SE, Rudolph DD, Kabara LL, Halsey KE, Hufnagel RB, Zhou J, Dolan DF, Glaser T. *Math 5* expression and function in the central auditory system. Mol Cell Neurosci. 2007 (E-publication ahead of print).

Schofield BR, Coomes DL. Auditory cortical projections to the cochlear nucleus in guinea pigs. Hearing Res 2005;199:89–102.

Shore SE, Moore JK. Sources of input to the cochlear granule cell region in the guinea pig. Hearing Res 1998;116:33–42.

Sekerkova G, Ilijic E, Mugnaini E. Toxicity of brodeoxyuridine during neurogenesis in rat cerebellum. J Comp Neurol 2004a;470:221–239. [PubMed: 14755513]

Sekerková G, Ilijic E, Mugnaini E. Time of origin of unipolar brush cells in the rat cerebellum as observed by prenatal bromodeoxyuridine labeling. Neuroscience 2004b;127:845–858.

Sekerková G, Ilijic E, Mugnaini E, Baker JF. Otolith organ or semicircular canal stimulation induces c-fos expression in unipolar brush cells and granule cells of cat and squirrel monkey. Exp Brain Res 2005;164:286–300. [PubMed: 15940501]

Sekerková G, Dino MR, Ilijic E, Russo M, Zheng L, Bartles JR, Mugnaini E. Postsynaptic enrichmemnt of Eps8 at dendritic shaft synapses of unipolar brush cells in rat cerebellum. Neuroscience 2007;145:116–129. [PubMed: 17223277]

Shepherd, GM. The Synaptic organization of the Brain. Oxford: Oxford University Press; 2004. p. 165-216.

Shore SE. Multisensory integration in the dorsal cochlear nucleus: unit responses to acoustic and trigeminal ganglion stimulation. Eur J Neurosci 2005;21:3334–3348. [PubMed: 16026471]

Shore SE, Vass Z, Wys NL, Altschuler RA. Trigeminal ganglion innervates the auditory brainstem. J Comp Neurol 2000;419:271–285. [PubMed: 10723004]

Shore SE, Zhou J. Somatosensory influence on the cochlear nucleus and beyond. Hear Res 2006;216–217:90–99.

Simpson JI, Hulscher HC, Sabel-Goedknegt E, Ruigrok TJ. Between in and out: linking morphology and physiology of cerebellar cortical interneurons. Prog Brain Res 2005;148:329–340. [PubMed: 15661201]

Slater, NT.; Rossi, DJ.; Jaarsma, D.; Mugnaini, E. Physiology and ultrastructure of unipolar brush cells in the vestibulocerebellum. In: Beitz, A.; Anderson, J., editors. Neurochemistry of the Vestibular System. Boca Raton, FL: CRC Press Inc; 1999. p. 287-301.

Smith PH, Rhode WS. Electron microscopic features of physiologically characterized, HRP-labeled fusiform cells in the cat dorsal cochlear nucleus. J Comp Neurol 1985;237:127–143. [PubMed: 4044890]

Spatz WB. Unipolar brush cells in the cochlear nuclei of a primate (*Callithrix jacchus*). Neurosci Lett 1999;270:141–144. [PubMed: 10462114]

Spatz WB. Unipolar brush cells in marmoset cerebellum and cochlear nuclei express calbindin. Neuroreport 2000;11:1–4. [PubMed: 10683819]

Spatz WB. Unipolar brush cells in the human cochlear nuclei identified by their expression of a metabotropic glutamate receptor (mGluR2/3). Neurosci Lett 2001;316:161–164. [PubMed: 11744227]

Spitzer NC. Electrical activity in early neuronal development. Nature 2006;444:707–712. [PubMed: 17151658]

Strominger, NL. The anatomical organization of the primate auditory pathways. In: Noback, CR., editor. Sensory systems in primates. New York: Plenum Press; 1978. p. 53-91.

Swanson, LW. Brain Maps: Structure of the Rat Brain. Amsterdam: Elsevier; 1992.

Terr LI, Edgerton BJ. Three-dimensional reconstruction of the cochlear nuclear complex in humans. Arch Otolaryngol Head Neck Surg 1985;111:495–501.

Tzounopoulos T, Kim Y, Oertel D, Trussel LO. Cell-specific, spike timing-dependent plasticities in the dorsal cochlear nucleus. Nature Neurosci 2004;7:719–725. [PubMed: 15208632]

Tzounopoulos T, Rubio ME, Keen JE, Trussel LO. Co-activation of pre- and postsynaptic signaling mechanisms determines cell-specific spike-timimg-dependent plasticity. Neuron 2007;54:291–301. [PubMed: 17442249]

Varecka L, Wu CH, Rotter A, Frostholm A. $GABA_A$/benzodiazepine receptor α α6 subunit mRNA in granule cells of the cerebellar cortex and cochlear nuclei: Expression in developing and mutant mice. J Comp Neurol 1994;339:341–352. [PubMed: 8132866]

Vetter, D.; Cozzari, C.; Hartman, BK.; Mugnaini, E. Choline acetylransferase in the rat cochlear nuclei: Immunolocalization with a monoclonal antibody. In: Merchán, MA.; Juiz, JM.; Godfrey, DA.; Mugnaini, E., editors. The Mammalian Cochlear Nuclei: Organization and Function. New York: Plenum Press; 1993. p. 279-290.NATO ASI Seriesvol 239

Víg J, Takács J, Abrahám H, Kovács GC, Hámori J. Calretinin-immunoreactive unipolar brush cells in the developing human cerebellum. Int J Dev Neurosc 2005;23:723–729.

Voogd, J.; Jaarsma, D.; Marani, E. The cerebellum: chemiarchitecture and anatomy. In: Bjorklund, A.; Hokfelt, T., editors. Handbook of Chemical Neuroanatomy. Vol. 12. Amsterdam: Elsevier; 1996. p. 1-369.

Wang VY, Rose MF, Zoghbi HY. Math 1 expression redefines the rhombic lip derivatives and reveals novel lineages within the brainstem and cerebellum. Neuron 2005;48:31–43. [PubMed: 16202707]

Webster, DB. An overview of mammalian auditory pathways, with emphasis on humans. In: Webster, DB.; Popper, AN.; Fay, RR., editors. The mammalian auditory pathway: Neuroanatomy. Berlin: Springer; 1992. p. 1-22.

Weedman DL, Ryugo DK. Projections from auditory cortex to the cochlear nucleus in rats: synapses on granule cell dendrites. J Comp Neurol 1996a;371:311–24. [PubMed: 8835735]

Weedman DL, Ryugo DK. Pyramidal cells in primary auditory cortex project to cochlear nucleus in rat. Brain Res 1996b;706:97–102. [PubMed: 8720496]

Weedman DL, Pongstaporn T, Ryugo DK. Ultrastructural study of the granule cell domain of the cochlear nucleus in rats: mossy fiber endings and their targets. J Comp Neurol 1996;369:345–60. [PubMed: 8743417]

Wei W, Zhang N, Peng Z, Houser CR, Mody I. Perisynaptic localization of the δ subunit –containing $GABA_A$ receptors and their activation by GABA spillover in the mouse dentate gyrus. J Neurosci 2003;23:10650–10661. [PubMed: 14627650]

Weinberg RJ, Rustioni A. A cuneocochlear pathway in the rat. Neuroscience 1987;20:209–219. [PubMed: 3561761]

Winsky L, Jacobowitz DM. Effects of unilateral cochlea ablation on the distribution of calretinin mRNA and immunoreactivity in the guinea pig ventral cochlear nucleus. J Comp Neurol 1995;354:564–582. [PubMed: 7608338]

Wolff A, Kuntzle H. Cortical and medullary somatosensory projections to the cochlear nuclear complex in the hedgehog tenrec. Neurosci Lett 1997;221:125–128. [PubMed: 9121680]

Wouterlood FG, Mugnaini E. Cartwheel neurons of the dorsal cochlear nucleus: A Golgi–electron microscopic study in rat. J Comp Neurol 1984;227:136–157. [PubMed: 6088594]

Wouterlood FG, Mugnaini E, Osen KK, Dahl AL. Stellate neurons in rat dorsal cochlear nucleus studied with combined Golgi impregnations and electron microscopy: synaptic connections and mutual coupling by gap junctions. J Neurocytol 1984;13:639–664. [PubMed: 6481413]

Wright DD, Ryugo DK. Mossy fiber projections from the cuneate nucleus to the cochlear nucleus in the rat. J Comp Neurol 1996;365:159–172. [PubMed: 8821448]

Wright DD, Blackstone CD, Huganir RL, Ryugo DK. Immunocytochemical localization of the mGluR1α metabotropic glutamate receptor in the dorsal cochlear nucleus. J Comp Neurol 1996;364:729–745. [PubMed: 8821458]

Yan XX, Garey LJ. Complementary distributions of calbindin, parvalbumin and calretinin in the cerebellar vermis of the adult cat. J Hirnforsch 1998;39:9–14. [PubMed: 9672106]

Yang Y, Saint Marie RL, Oliver DL. Granule cells in the cochlear nucleus sensitive to sound activation detected by fos protein expression 2005;136:865–882.

Yao W, Godfrey DA, Levey AI. Immunolocalization of muscarinic acetylcholine subtype 2 receptors in rat cochlear nucleus. J Comp Neurol 1996;373:27–40. [PubMed: 8876460]

Yao W, Godfrey DA. Vesicular acetylcholine transporter in the rat cochlear nucleus: an immunohistochemical study. J Histochem Cytochem 1999;47:83–90. [PubMed: 9857215]

Young, ED.; Oertel, D. Cochlear nucleus. In: Shepherd, GM., editor. The Synaptic Organization of the Brain. Oxford: Oxford University Press; 2004. p. 125-163.

Zervas M, Millet S, Ahn S, Joyner AL. Cell behaviors and genetic lineages of the mesencephalon and rhombomere 1. Neuron 2004;43:345–357. [PubMed: 15294143]

Zhao HB, Parham K, Ghoshal S, Kim DO. Small neurons in the vestibular nerve root project to the marginal shell of the anteroventral cochlear nucleus in the cat. Brain Res 1995;700:295–298. [PubMed: 8624725]

Zhan X, Pongstaporn T, Ryugo DK. Projections of the second cervical dorsal root ganglion to the cochlear nucleus in rats. J Comp Neurol 2006;496:335–348. [PubMed: 16566003]

Zhan X, Ryugo DK. Projections of the lateral reticular nucleus to the cochlear nucleus in rats. J Comp Neurol 2007;504:583–588. [PubMed: 17701985]

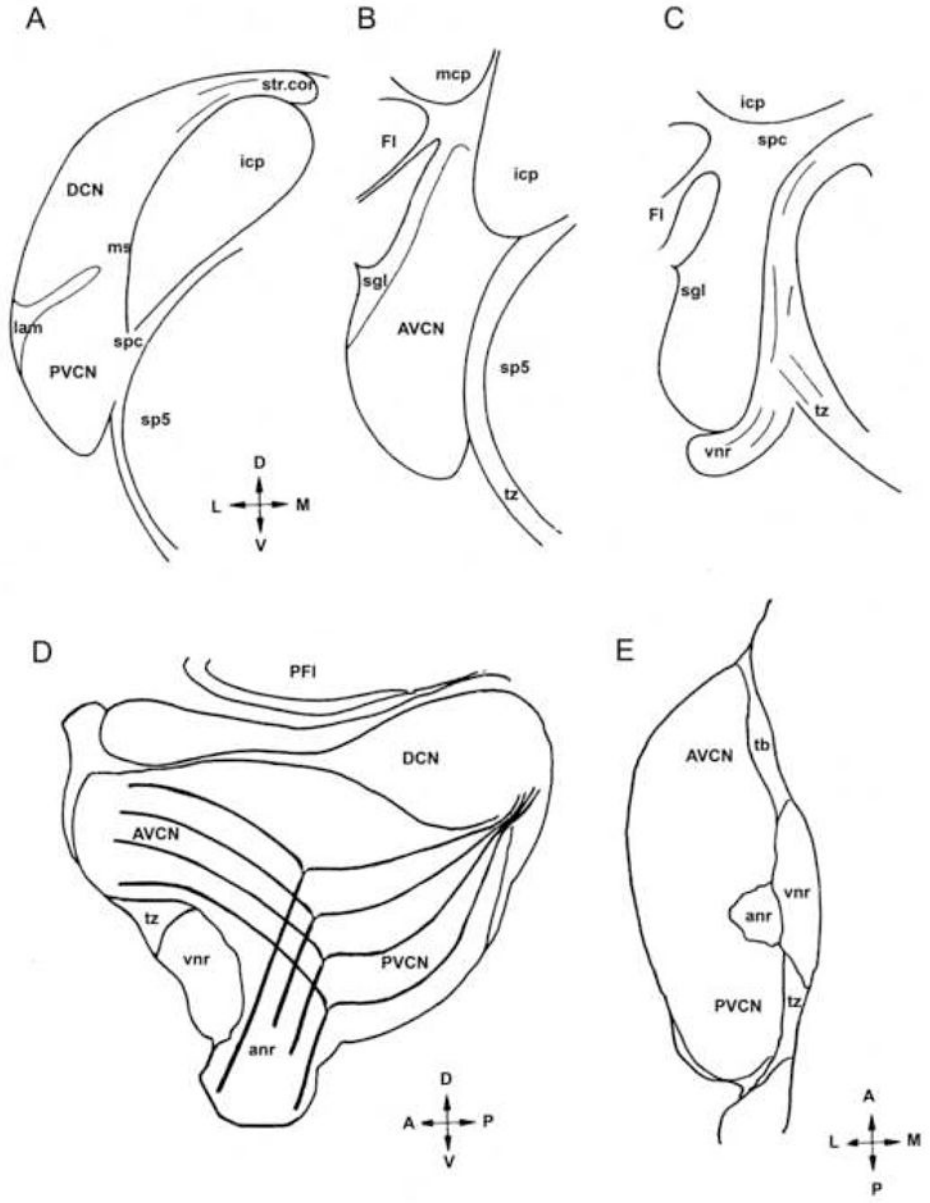

Fig. 1. Schematic diagram shows the rat CN in coronal (A–C), sagittal (D) and horizontal (E) sections

Auditory nerve root (anr); anteroventral cochlear nucleus (AVCN); cochlear nerve root with tonotopically arranged branching fibers (cnr); flocculus (Fl); inferior cerebellar peduncle (icp); lamina (lam); medial sheet (ms); middle cerebellar peduncle (mcp); spinal tract (sp5); posteroventral cochlear nucleus (PVCN); superficial granular layer (sgl); strial corner (str. cor.); supeduncular corner (spc); trapezoid body (tz); vestibular nerve root (vnr); arrows indicate dorsal, ventral, medial and lateral axes.

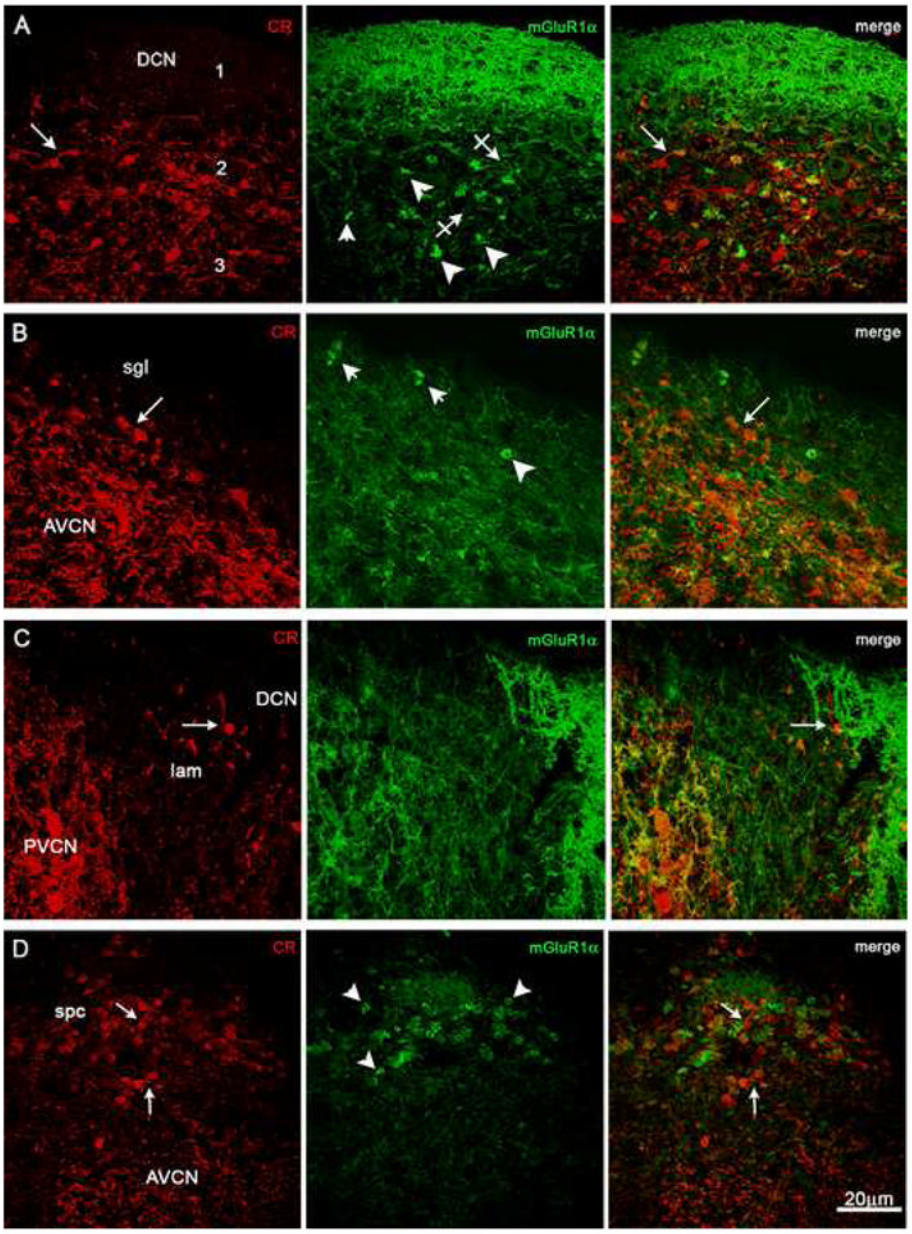

Fig. 2. Two-color immunofluorescence micrographs from CN sections stained with antisera to calretinin (CR) and mGluR1α

A variety of immunoreactive neuronal cells and fibers are present throughout the CN and partly obfuscate immunostained UBCs, which are present at higher densities in DCN and spc than in sgl and lamina. Arrows indicate CR^+ UBCs and crossed arrows $mGluR1\alpha^+$ UBCs; arrowheads point to putative brushes of $mGluR1\alpha^+$ UBCs. Row A: Midportion of the DCN in sagittal section. Row B: Portion of the superficial granular layer (sgl) overlaying the AVCN. Row C: Lateral portion of the lamina (lam) flanked by PVCN and DCN. Row D: Subpeduncolar corner (spc) above the AVCN. Magnification bar = 20 μm.

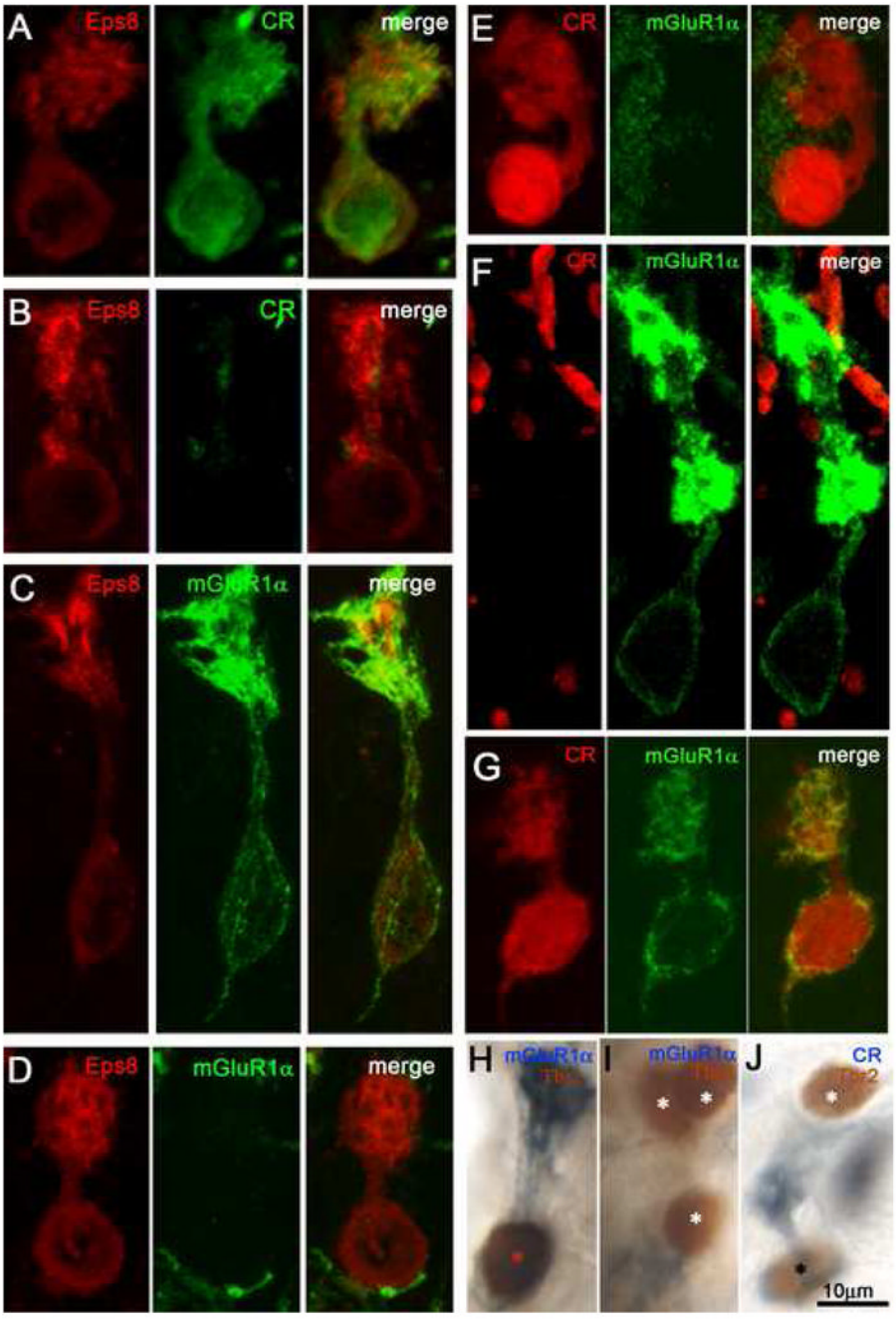

Fig. 3. Laser scanning confocal immunofluorescence micrographs (rows A–G) and brightfield, two-color immunoreaction (panels H–J) demonstrate chemical heterogeneity of UBCs from various regions of the CN. Color channels are indicated in the individual panels

Row A: $Eps8^+/CR^+$ UBC from DCN. Row B: $Eps8^+/CR^-$ UBC from DCN. Row C: $Eps8^+/mGluR1\alpha^+$ UBC from spc. Row D: $Eps8^+/mGluR1\alpha^-$ UBC from DCN. Row E: $CR^+/mGluR1\alpha^-$ UBC from border of DCN and sgl. Row F: $CR^-/mGluR1\alpha^+$ UBC from PVCN. Row G: UBC immunopositive for both CR and mGluR1α, from anr. Panel H: Tbr2+/$mGluR1\alpha^+$ UBC from tz. Panel I: Cluster of three $Tbr2^+/mGluR1\alpha^-$ UBCs from the DCN. Panel J: Two UBCs, one of which is $Tbr2^+/CR^+$ and the other $Tbr2^+/CR^-$ from sp5. Asterisks in panels H–J indicate Tbr2-immunoreactive UBC nuclei. Magnification bars = 10 μm.

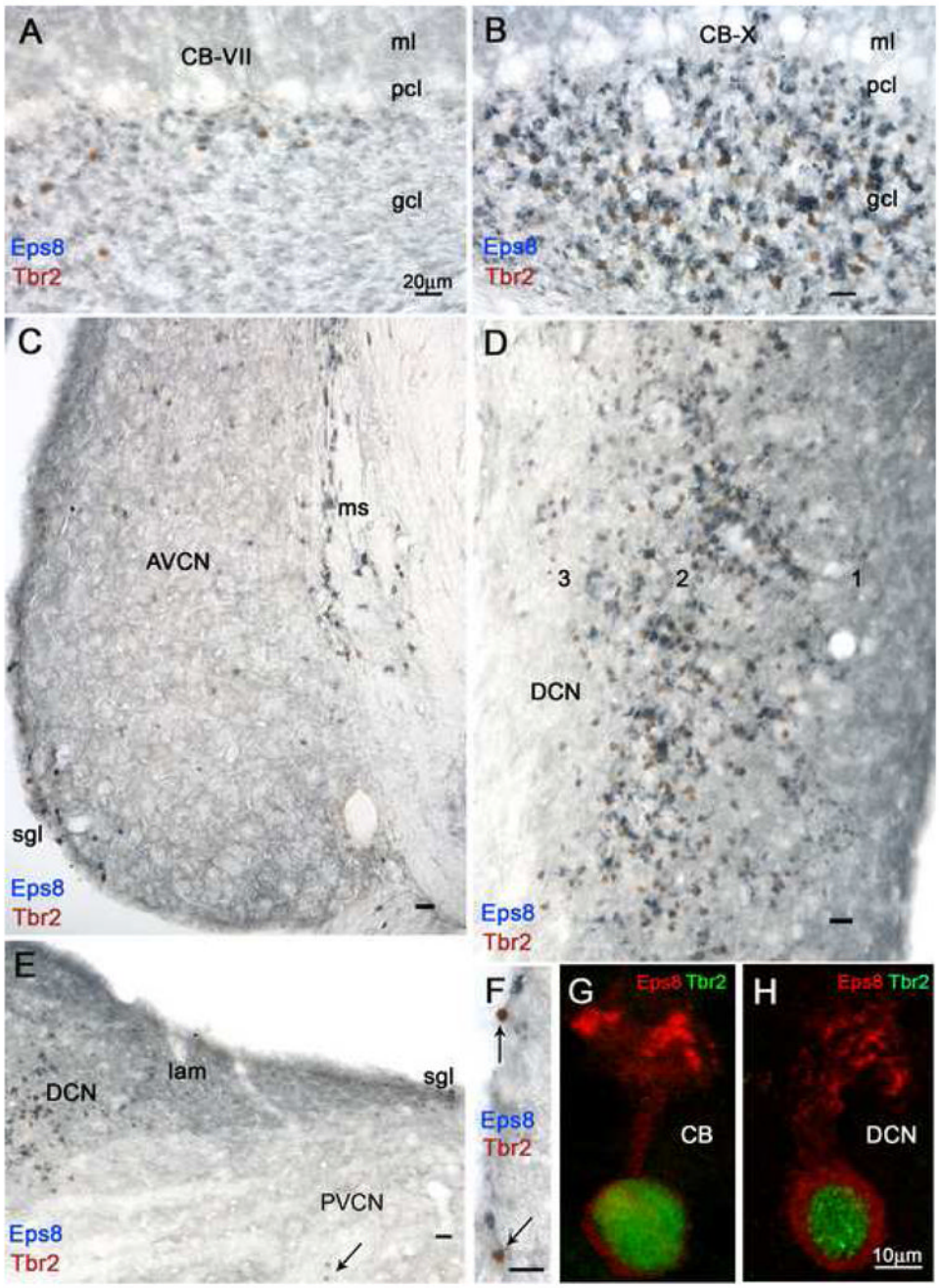

Fig. 4. Two-color brightfield micrographs (panels A–F) from sections immunostained with antisera to Eps8 (blue) and Tbr2 (brown) show varying densities of UBCs in folia of lobules VII (CB-VII) and X (CB-X) of the cerebellar cortex and in regions of the CN. Panels G and H (two-color immunofluorescence) show individual UBCs from cerebellum CB) and DCN and illustrate cytoplasmic staining by Eps8 antiserum (red) and nuclear staining by Tbr2 antiserum (green)

A and B: Even at this low magnification it is evident that the granular layers (gcl) of the two lobules contain different densities of intensely $Eps8^{+}$ neuropil structures and $Tbr2^{+}$ nuclei, identified at higher magnification as brushes and nuclei of UBCs, respectively (see panel G). Granule cell glomeruli and molecular layer (ml) parallel fibers are weakly Eps8 immunoreative; the Purkinje cell layer (pcl) is unstained. C: This coronal section of the AVCN demonstrates higher density of UBCs in the medial sheet (ms) than in the superficial granular

layer (sgl) and the magnocellular AVCN; moreover, the density of UBCs is higher in rostral than ventral parts of AVCN. D: Detail from a coronal section tilted 90° shows high density of UBCs in layer 2 and the polymorphic layer 3 of the DCN, while granule cell glomeruli and molecular layer 1 parallel fibers are weakly $Eps8^{+}$. E: The lamina (lam) shows moderate Eps8 staining of granule cells and glomeruli, while numerous UBCs are present in the adjacent DCN and one UBC (arrow) is present in the magnocellular PVCN. F: Two UBCs (arrows) and several granule cells (arrowhead) in the superficial granular layer of AVCN. G and H: UBCs in the granular layer of the cerebellum (CB) and DCN. Magnification bars A–F = 20 μm; G, H = 10 μm.

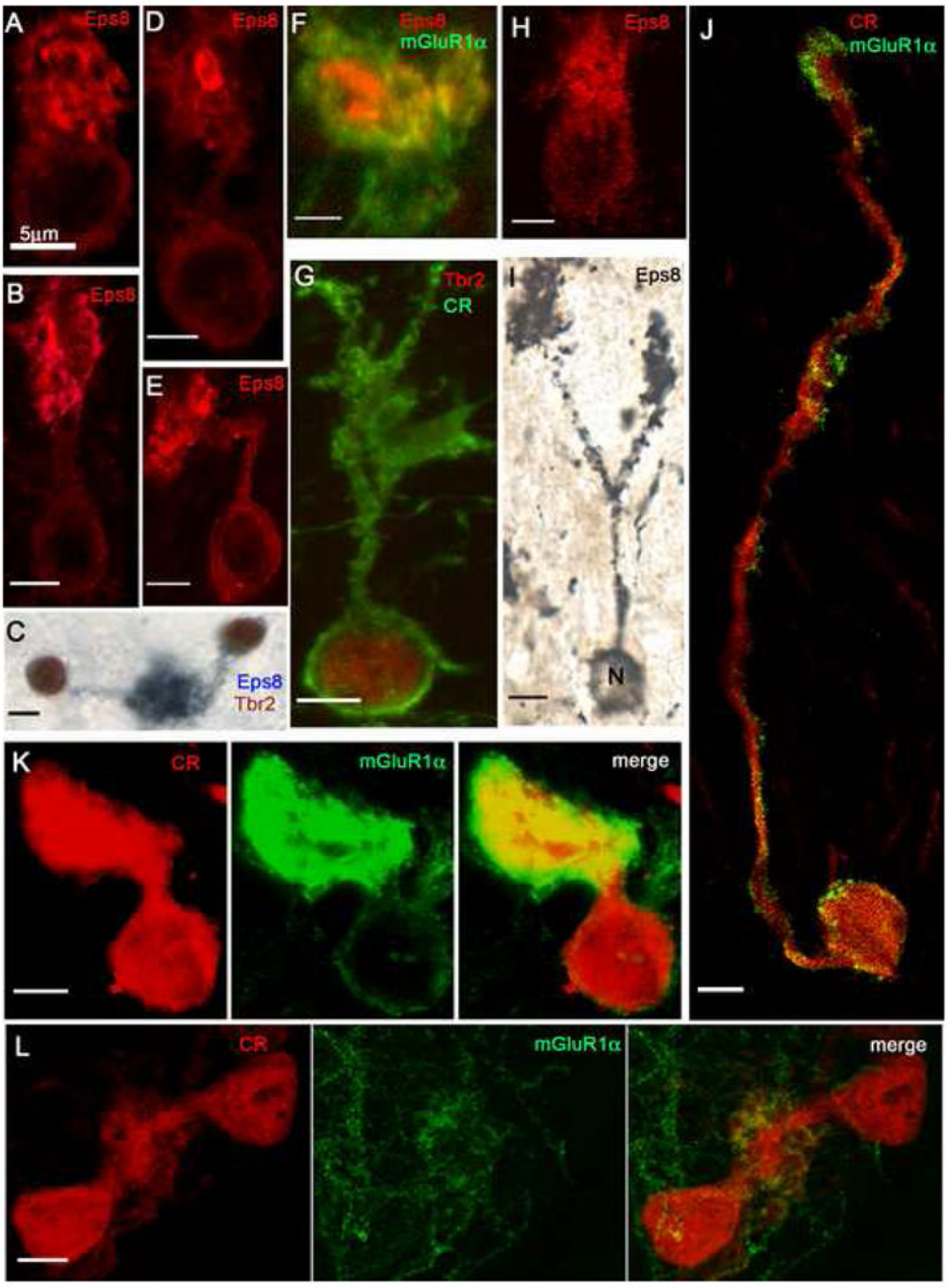

Fig. 5. Morphological UBC variants in the CN demonstrated by laser confocal immunofluorescence (panels A, B, D, E, H, K, L, and J) and brightfield microscopy (panels C and I)

A: The bulbous brush of this UBC arises directly from the cell body and contains multiple, fragmented Eps8$^+$ foci. B: The elongated brush of this UBC arises from a short and straight dendritic stem and contains variously shaped Eps8$^+$ foci. C: Two UBCs, double-labeled with Eps8 and Tbr2, contribute brushes to the same glomerulus. D: UBC brush with large, ring-like Eps8$^+$ focus. E: UBC with sharply bent dendritic stem. F: Detail of an UBC brush (identified by peripheral staining with mGluR1α) that contains two large Eps8$^+$ foci. G: This CR$^+$/Tbr2$^+$ UBC shows a loose array of brush dendrioles. H: This UBC, stained with Eps8, emanates dendrioles from different parts of the cell body (compare with panel A). I: This UBC, stained

with a silver-enhanced Eps8/DAB protocol, shows two brushes formed by branches of a long dendritic stem. J: $CR^+/mGluR1\alpha^+$ UBC emits an unusually long dendrite that forms a small, elongated brush. Row K: This UBC has a very short dendrite and a large, compact brush; dual immunostaining of both cell body and brush indicates mixed, $CR^+/mGluR1\alpha^+$ phenotype. Row L: The brushes of two $CR^+/mGluR1\alpha^-$ UBCs merge into the same glomerular array. Magnification bars = 5 μm.

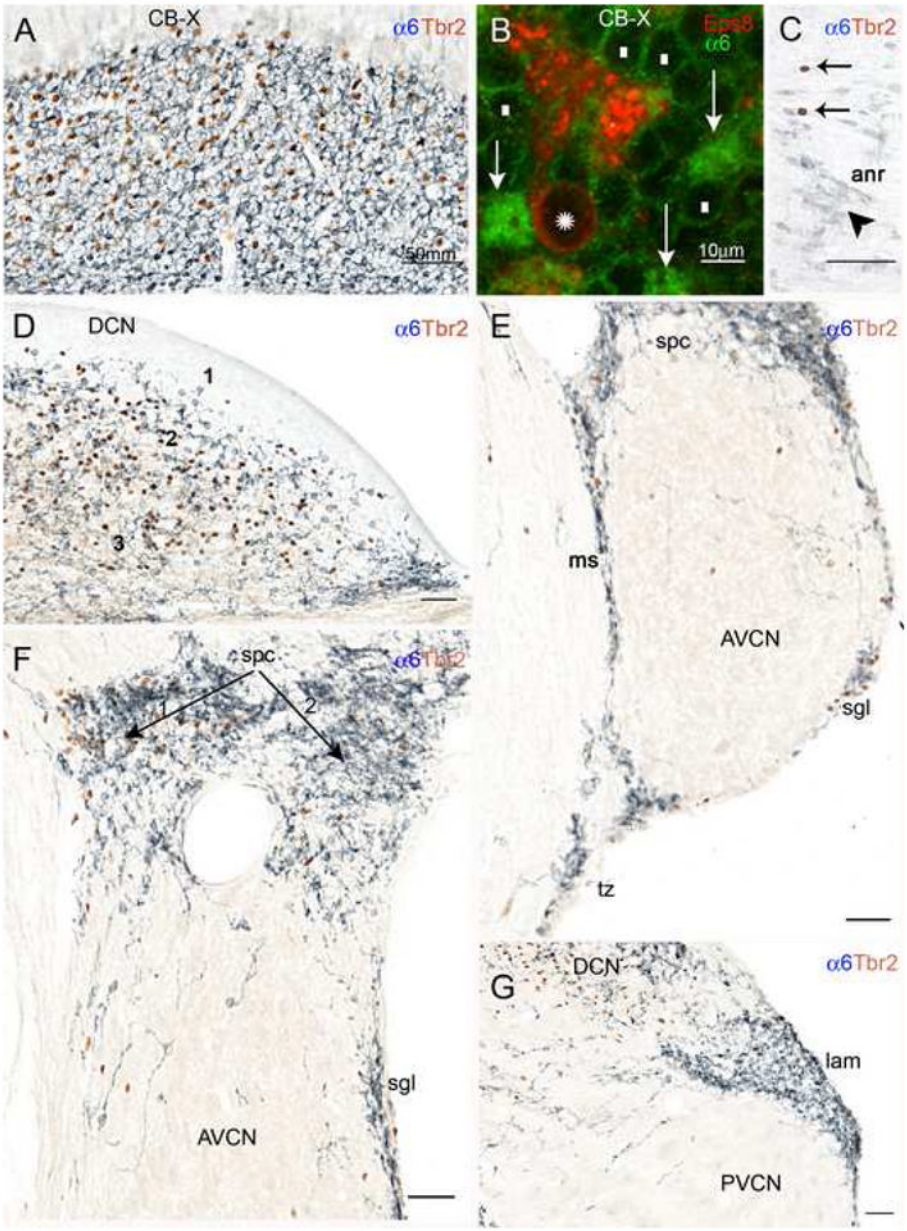

Fig. 6. Double-labeling with antisera to either Eps8 or Tbr2 and the α6 subunit of the $GABA_A$ receptor with immunofluorescence (panel B) and brightfield microscopy (all other panels) proves that UBCs and granule cells are codistributed within the CN and in neighboring territories. In the brightfield micrographs UBC nuclei are stained red/brown, while the cytoplasm is unstained; by contrast, the cell bodies and glomerular dendrites of granule cells appear as pale blue ringlets with a clear nucleus and deeper blue neuropil areas, respectively

A: Detail from the transition between the cerebellar flocculus and paraflocculus shows high densities of UBC and granule cell immunoreactivities. B: This standard immunofluorescence micrograph shows that the cerebellar UBC (asterisk over the nucleus) labeled by the UBC cell class marker Eps8 lacks α6 immunoreactivity; granule cell bodies (white rectangles) show weak α6 immunoreactivity along the plasma membrane, but their dendritic tips in the glomeruli (arrows) are intensely stained. C: Detail from the cochlear nerve root showing several granule cells (arrowheads) and the nuclei of two UBCs (arrows); D: The DCN contains high densities

of UBCs and granule cells in layer 2 and the polymorphic layer 3, but not in the molecular layer 1. E: UBCs and granule cells are present in the medial sheet (ms), superficial granular layer (sgl), and subpeduncular corner (spc), and also in the trapezoid body (tb), and the magnocellular AVCN. F: In the subpeduncular corner the density of granule cells is homogenously high, while UBCs are clustered in the area indicated by arrow 1, and sparse in the area labeled by arrow 2. Scattered granule cells and UBCs are present in the magnocellular AVCN. G: The lamina contains numerous granule cells, but rare UBCs. Scattered granule cells and UBCs are present in the magnocellular PVCN. Magnification bars A, C–G= 50 μm; B= 10 μm.